

Eddy Current Brake Design for Operation with Extreme Back-drivable Eddy Current Motor:

Final TEAM 16

Hollowell, Thomas Culver; Kahl, Justin Tyme; Stanczak, Matthew Don; Wang, Yizhou
2010 Mechanical Engineering Undergraduates

Traditional electric motors have a tradeoff between high torque and low rotor inertia. The goal of this project is to eliminate using the physics of eddy currents. We have created an eddy current brake which uses the same eddy current effect as an eddy current motor but is simpler to build. We hope to learn the effect of stator spacing, magnet size and shape, number of magnets, magnet radius, and phase angle have on braking force. This information will be used by another team to create an eddy current motor.

1 EXECUTIVE SUMMARY

The document reports the progress of Team 16's Eddy Current Brake design. This project has been motivated by the hypothesis that the torque-inertia trade-off existing in traditional electric motors can be eliminated by use of permanent magnets and the phenomena of eddy currents. Customer requirements have been translated into engineering specifications consisting of maximizing torque while minimizing rotor inertia. This specification has been further condensed into a performance index which is maximized.

An alpha prototype has been produced in order to inform the final design and also to perform preliminary performance calculations. From this model it was determined that large loads will be supported and therefore a closed mechanical structure is required. Further, elementary functional relationships between brake performance and geometric configurations have been developed.

A final bench top eddy current brake test apparatus has been produced. Experimentation has been performed. The current experimental results suggest that the eddy current motor would have to be driven at high speeds to show significant performance advantages over electric motors. This result may however be negated by more rigorous geometric configuration experimentation resulting in optimized eddy current brake/motor configuration.

TABLE OF CONTENTS

2	PROBLEM DESCRIPTIONS	– page 5
3	ENGINEERING SPECIFICATION	- page 5
4	THEORETICAL DERIVATIONS	– page 5
	4.1 Generation of Eddy Currents	– page 5
	4.2 Eddy Current Brake Model	– page 6
	4.3 Governing Equation of Motion	– page 7
5.	DESIGN PARAMETER OPTIMAZATION	– page 8
	5.1 Rotor Disc Clearance	– page 8
	5.2 Rotor Material	– page 8
	5.3 Rotor Disc Thickness	– page 8
	5.4 Rotor Disc Radius	– page 8
	5.5 Stator Permanent Magnet Array Orientation	– page 9
6	PERFORMANCE EVALUATIONS	– page 9
	6.1 Initial ECB Performance Evaluation	– page 10
	6.1.1 <i>Experimental Setup and Calculation</i>	– page 10
	6.1.2 <i>Experiment procedure</i>	– page 12
7	CONCEPT GENERATIONS AND EVALUATION	– page 12
	7.1 Stator	– page 12
	7.1.1 <i>Concept Overviews</i>	– page 12
	7.1.2 <i>Concept Evaluation</i>	– page 14
	7.2 Rotor	– page 15
	7.2.1 <i>Concept Overviews</i>	– page 15
	7.2.2 <i>Concept Evaluation</i>	– page 17
	7.3 Mechanical Structure	– page 18
	7.3.1 <i>Concept Overviews</i>	– page 18
	7.3.2 <i>Concept Evaluation</i>	– page 19
8	PARAMETER ANALYSES ALPHA DESIGN	– page 19
	8.1 Definition of Parameters	– page 19
	8.2 Stator Air Gap	– page 21
	8.3 Stator Phase Angle	– page 24
	8.4 Magnetic Array Radius	– page 26
	8.5 Quantity of Stator Magnets	– page 27
	8.6 Vizimag Analysis	– page 28
	8.6.1 <i>Procedure</i>	– page 28
	8.6.2 <i>Magnet spacing</i>	– page 29
	8.6.3 <i>Stator Spacing</i>	– page 29
	8.7 Summary of Material Selections	– page 31
	8.8 Summary of Manufacturing Process	– page 31
9	SAFETY ANALYSES	– page 31
	9.1 Open-Structure Housing	– page 31
	9.2 Closed-Structure Housing	– page 32
	9.3 Friction	– page 34
10	FINAL DESIGN	– page 34
11	FABRICATION PLAN	– page 35

11.1 Manufacturing Plan	– page 35
<i>11.1.1 Handle</i>	<i>– page 36</i>
<i>11.1.2 Stator Holder</i>	<i>– page 36</i>
<i>11.1.3 Rotating Stator</i>	<i>– page 36</i>
<i>11.1.4 Rotating Stator Axle</i>	<i>– page 36</i>
<i>11.1.5 Rotors</i>	<i>– page 37</i>
<i>11.1.6 Spacer</i>	<i>– page 37</i>
<i>11.1.7 Spacer for Rotor Plate</i>	<i>– page 38</i>
<i>11.1.8 Stationary Stator</i>	<i>– page 38</i>
11.2 Assembly	– page 38
<i>11.2.1 Sub-assemblies</i>	<i>– page 38</i>
<i>11.2.2 Full Assembly</i>	<i>– page 46</i>
12 VALIDATION APPROACH	– page 47
12.1 Experimental setup, procedure and measurements	<i>– page 47</i>
12.2 Validation results	<i>– page 47</i>
12.3 Comparison of performance indexes	<i>– page 49</i>
13 DESIGN CRITIQUE	– page 49
14 RECOMMENDATIONS	– page 49
15 CONCLUSIONS	– page 50
16 ACKNOWLEDGEMENTS	– page 50
17 INFORMATION SOURCES	– page 50
17.1 Benchmarking	<i>– page 50</i>
17.2 Patent Search	<i>– page 50</i>
REFERENCES	– page 51
APPENDIX A: Gantt Chart	– page 52
APPENDIX B: QFD	– page 53
APPENDIX C: Team Member Autobiographies	– page 54
APPENDIX D: DESIGN CHANGES SINCE DR3	– page 56
APPENDIX E: BILL OF MATERIALS	– page 57
APPENDIX F: MATERIAL SELECTION	– page 58

2 PROBLEM DESCRIPTIONS

Haptic feedback devices use electric motors to apply feedback forces to the user, but they are less than ideal for this task. To get the high torque necessary to simulate virtual objects the motor must have a large rotor. The large rotor however causes problems when the feeling of free space is desired because the user feels the inertia of the rotor. Our sponsor, Professor Gillespie, has asked us to explore the possibility of using an eddy current brake to accomplish lower inertia and higher torque than provided by a traditional electric motor. The proposed eddy current brake will work by phasing permanent magnets mounted on the stator. So when full braking is required opposite poles are located across from each other which would create a large magnetic flux through the conductive rotor, generating a torque. When no torque is required like poles will be located across from each other so that there is no magnetic flux going through the rotor. This phasing of magnetic poles will provide a continuous range of output torque between maximum backdriveability and maximum torque.

3 ENGINEERING SPECIFICATION

Motor torque and backdrivability are the two main customer requirements. Cost is a minor requirement because this is a new conceptual design. Evaluation of the brake performance is thus based on the magnitude of the torque it can generate to resist the rotor's motion and maximum backdrivability. Thus, a zero torque together with a minimum inertia when the brake is off is required. Therefore, the corresponding engineering specifications are torque generated in both on and off cases and the inertia of the rotor. Also, parameters that contribute to these engineering specifications were listed: the strength of magnetic field, device geometries and material properties. We confront these parameters in the physical derivations of our model. A detailed QFD is attached in Appendix B showing the transformation from user demands into engineering specifications. Further, interaction of these parameters and their relative importance was examined. A full understanding of our engineering specifications improves our decisions in designing our prototype.

We have shown two competitors in the market. However, both of them are using electromagnetic coils instead of permanent magnets so competitor benchmarking is limited in its usefulness (See Appendix B for QFD).

4 THEORETICAL DERIVATIONS

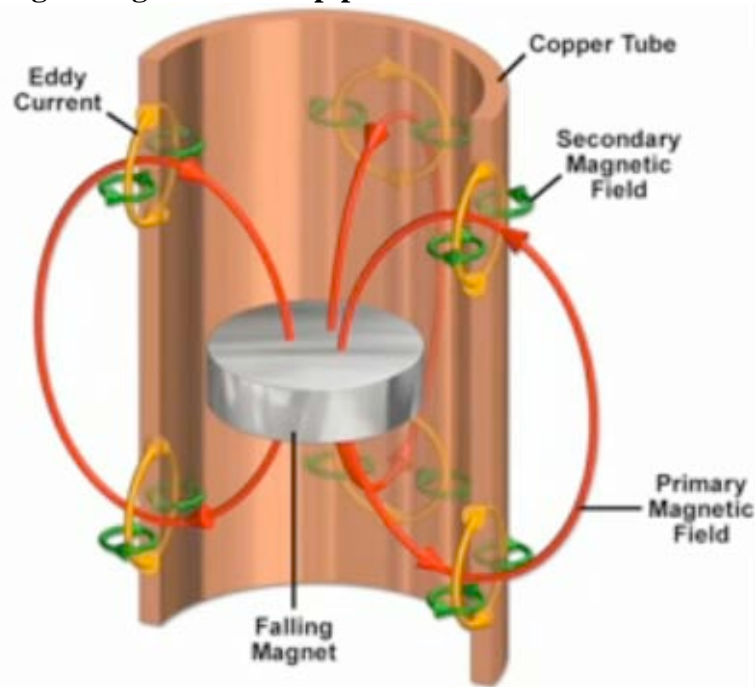
In this section the physics governing the dynamics of eddy currents are investigated and a simple model of our system is developed.

4.1 Generation of Eddy Currents

Eddy currents are the currents that are generated because of a change in time and space of magnetic flux passing through conducting non ferrous metals. This phenomenon is governed by both Faraday's law of induction and Lenz's Law. Faraday's Law of Induction states that any change in the magnetic environment of a coil of conducting wire will cause a voltage (electromagnetic force, or ϵmf) to be induced in the coil. Lenz's Law states that when an ϵmf is generated by a change in magnetic flux, according to Faraday's law, the polarity of the induced ϵmf is such that it produces a current whose magnetic field opposes the change which produced

it. Figure 1 shows a typical example of the generation of eddy currents. When a magnet falls through a copper pipe, there is some change of magnetic flux in a certain portion of metal. Simultaneously, eddy currents are generated around the primary magnetic field. The secondary magnetic field (or induced magnetic field) is always opposing the change of flux so that the resulting Lorentz's force magnets descent. Although the exact eddy current profiles are quite complicated and somehow undetermined but deterministic, the effects are always clear, opposing the motion, or the flux-cutting velocity.

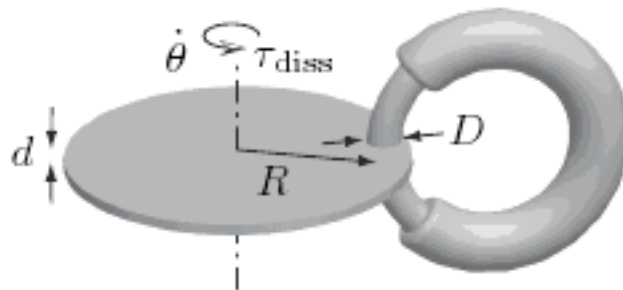
Figure 1: Illustration of magnetic field lines arrangement and generation of eddy currents when a magnet falling through a metallic pipe.



4.2 Eddy Current Brake Model [1]

The eddy current brake implements the idea introduced above to generate a torque sufficiently large that resists the rotational motion of wheels. Figure 2 shows the schematic diagram of a simple eddy current brake with only one magnet around it. The subsequent analysis is based on this simple model.

Figure 2: Schematic diagram of eddy current brake (disc brake) [1].



The disk and the ring in this figure represent a rotating wheel and a magnet whose field goes through the edge of the wheel respectively. Similar to the example of falling magnet in a metallic pipe, a braking torque is generated on the disk resisting the rotational motion. The magnitude of the braking torque, τ_{diss} [N·m] can be theoretically derived to be a function of the number of magnets around the wheel, n [#], the specific conductivity of the material, σ [$\Omega^{-1} \cdot \text{m}^{-1}$], the diameter of the magnet core, D [m], the thickness of the disk, d [m], the magnetic field, B [T], the effective radius, R [m], and the instantaneous angular velocity, $\dot{\theta}$ [rad/s]:

$$\tau_{diss} = n \frac{\pi\sigma}{4} D^2 d B^2 R^2 \dot{\theta} \quad \text{Eqn. (1)}$$

The torque should vary linearly with angular velocity. However, the equation shown above is given under the assumption that the primary magnetic field is sufficiently greater than the induced magnetic field. Experiments have shown that the braking torque does vary linearly with velocity at low speeds. [2],[3],[4] Thus, the ECB dynamics are simplified and will be modeled as a linear damper in the subsequent analysis.

4.3 Governing Equation of Motion

The free response of the rotating disk at a certain initial condition can be modeled in a second-order differential equation by Newton's Second Law:

$$I\ddot{\theta} + b\dot{\theta} = 0, \quad \text{with } \theta = 0 \\ \dot{\theta} = \omega_0 \quad \text{Eqn. (2)}$$

Here b represents the integration of variables before the angular velocity term in Equation (3) as a damping coefficient and, I is the moment of inertia of the disk. Explicitly, they are:

$$b = n \frac{\pi\sigma}{4} D^2 d B^2 R^2 \quad \text{Eqn. (3)}$$

$$I = \frac{1}{2} \rho d \pi R^4 \quad \text{Eqn. (4)}$$

When formulating the above equation, we overlook any other viscous or static frictions existing in the system because they are only secondary effects. By solving the equation of motion, the angular velocity can be obtained to be:

$$\dot{\theta} = \omega_0 e^{-(b/I)t} = \omega_0 e^{-(1/\tau)t} \quad \text{Eqn. (5)}$$

The time constant, τ [s] is therefore the ratio of the moment of inertia of the disk to the effective damping coefficient:

$$\tau = I/b = 2\rho R^2 / n\sigma D^2 B^2 \quad \text{Eqn. (6)}$$

It not only captures the brake performance, but also shows the tradeoffs that maximize the damping for the smallest inertia. A small value is expected for the time constant which means it takes less time for a wheel to stop rotating. Equation 6 gives the ideal design guideline that qualitatively helps us optimize the brake performance before any experimental verification.

5. DESIGN PARAMETER OPTIMAZATION

The design of an eddy current brake reduced to five optimization problems which are discussed in the proceeding sections.

5.1 Rotor Disc Clearance

The rotor disc clearance must be optimized to maximize torque when the brake is on and maximize backdrivability when the brake is off. The tradeoffs of this optimization are: maximum torque requires minimum clearances while maximum backdrivability may have a clearance threshold where within the eddy currents cannot be eliminated due to the parabolic shape of the magnetic field lines in the off case. This optimization will be largely conducted experimentally.

5.2 Rotor Material

The material of the rotor disc must also be optimized in order to minimize the time constant, τ and minimize the disc's moment of inertia, I . There are two strong candidates in our selection of material which are copper and aluminum. This evaluation is based on the qualitative result of Equation 7. In order to minimize the time constant, we must choose the smallest ratio of density, ρ to conductivity, σ from all the materials available. We have evaluated the ratios for a number of possible commercial materials. We find that copper and aluminum rank top. The ratio for copper is calculated to be $1.5 \cdot 10^{-4} \text{ kgm}^2/\text{S}$ and for aluminum is $0.76 \cdot 10^{-4} \text{ kgm}^2/\text{S}$. Therefore, we plan to use aluminum as the material for our rotating disk in the prototype in order to achieve better brake performance.

$$\tau = I/b = 2\rho R^2/n\sigma D^2 B^2 \quad \text{Eqn. (7)}$$

Table 1: Comparison between copper and aluminum as the material for the rotating disk.

	Density [kg/m ³]	Specific Conductivity [S/m]	Ratio [kgm ² /S]
Copper	$8.9 \cdot 10^3$	$58.0 \cdot 10^6$	$1.5 \cdot 10^{-4}$
Aluminum	$2.7 \cdot 10^3$	$35.5 \cdot 10^6$	$0.76 \cdot 10^{-4}$

5.3 Rotor Disc Thickness

The thickness of the rotor disc, d , must also be optimized in order to minimize the time constant, τ and minimize the disc's moment of inertia, I . The inertia of the disc is linearly proportional to the thickness (Equation 8), so minimizing the disk radius minimizes the disk inertia. The time constant does not depend on the disc thickness (Equation 9). Thus, the optimization problem reduces to minimizing disc thickness while maintaining enough structural rigidity.

$$I = \frac{1}{2} \rho d \pi R^4 \quad \text{Eqn. (8)}$$

$$\tau = I/b = 2\rho R^2/\sigma D^2 B^2 \quad \text{Eqn. (9)}$$

5.4 Rotor Disc Radius

The radius of the rotor disc, R , must also be optimized in order to minimize the time constant, τ and minimize the disc's moment of inertia, I . The inertia of the disc is proportional to the radius

to the fourth power (Equation 10), so minimizing the disk radius minimizes the disk inertia. The functionality of the time constant on the disc radius isn't as clear. Equation 11 shows that the time constant is proportional to the radius squared, however the magnetic flux, $\phi(R)$, is also a function of the disc radius because the larger the radius the more magnets can be mounted and thus the stronger the magnetic field. This functionality of the magnetic field on the disc radius is unknown and may only be evaluated experimentally (Equation 12). Thus, optimization of the rotor disc radius poses a design challenge due to incomplete governing mathematical relations.

$$I = \frac{1}{2} \rho d \pi R^4 \quad \text{Eqn. (10)}$$

$$\tau = I/b = 2\rho R^2 / \sigma D^2 B^2 n \quad \text{Eqn. (11)}$$

$$\phi(R) = BD(R)n(R) \quad \text{Eqn. (12)}$$

5.5 Stator Permanent Magnet Array Orientation

The orientation of the permanent magnets on the stator must also be optimized in order to maximize the strength of the eddy currents. This optimization will be largely experimental and will evaluate several design variables including:

- Whether it is best to use many small magnets, or few large magnets.
- Circumferentially versus radially mounted magnets.
- Magnetic pole patterns including N-S-N-S-N-S versus N-S-none-N-S-none...

Since these design variables will be evaluated experimentally it will be advantageous to have a test apparatus that incorporates flexible stator permanent magnet array orientations.

6 PERFORMANCE EVALUATIONS

The customer requires that the permanent magnet eddy current brake (ECB) produce large brake torques when “on” and low brake torques when “off”. In addition, the customer requires that the brake torque be continuously variable between the extreme on and off cases. Further, it is required that the mass moment of inertia of the rotor be minimized. Finally, it is required that the ECB have torque and speed sensing capabilities. These customer requirements allow for simulation of both free space and massivity in haptic interfaces. Previously, in section 3.2 the aforementioned customer requirements were transformed into engineering specifications.

Currently, the ECB engineering specifications have been further transformed into a *Performance Index, PI* (Equation 13) which will allow for evaluation of the ECB's performance and the extent to which it meets the customer requirements.

$$PI = \frac{\tau_{max}}{\tau_{min} + I * \ddot{\theta}} \quad \text{Eqn. (13)}$$

This performance index captures the two extremes that needed to be maximized. Specifically, we seek to maximize ECB-ON torque and second, while maximizing backdriveability (or minimizing ECB-OFF torque and rotor inertia). Further, it is intuitive to consider the torque produced by the angular acceleration of the rotor as opposed to its inertia alone. As in the previously proposed PI, some reference parameters were selected. A reference angular acceleration was chosen by estimating the fastest someone could rotate their wrist π radians to be 0.25 seconds and further we estimated that the hand underwent constant acceleration followed by

constant deceleration. Therefore, the maximum angular acceleration that the ECB will undergo is approximately 200 radians/s^2 . The minimum angular acceleration the ECB will undergo is 0 radians/s^2 . Therefore the reference angular acceleration was chosen as the average of these extremes.

This performance index has the added advantage of being non-dimensional. Further, if the ECB-OFF torque is zero then the denominator reduces to the torque due to accelerating the rotor, thus capturing one of the key design requirements. If the ECB-ON torque is maximized the *PI* increases, but if increasing the ECB-ON torque comes at the cost of increasing the ECB-OFF torque or the rotor inertia torque then no net performance gain is experienced. This, trade-off relationship is central to a functional performance index and is well captured by the current performance index definition.

6.1 Initial ECB Performance Evaluation

A rapid prototype for use in experiments has been developed. This physical prototype will enable evaluation of different ECB component concepts via experimentation. Some initial evaluations have been made. The performance of the physical prototype has been compared to the performance of several different aerospace quality DC motors produced by *Maxon Motors*, by means of a “rough and dirty” bench top test.

6.1.1 Experimental Setup and Calculation

The experimental setup consisted of hanging a known weight on the axle of the physical prototype ECB (Figure 3) rotor acting as a known moment. The weight was allowed to free fall and after one full rotation of the rotor (ensuring transients have disappeared) the time for a second full rotor rotation was timed with a stop watch. Figure 4 shows a free body diagram of the experimental setup.

Figure 3: Experimental set-up and physical model

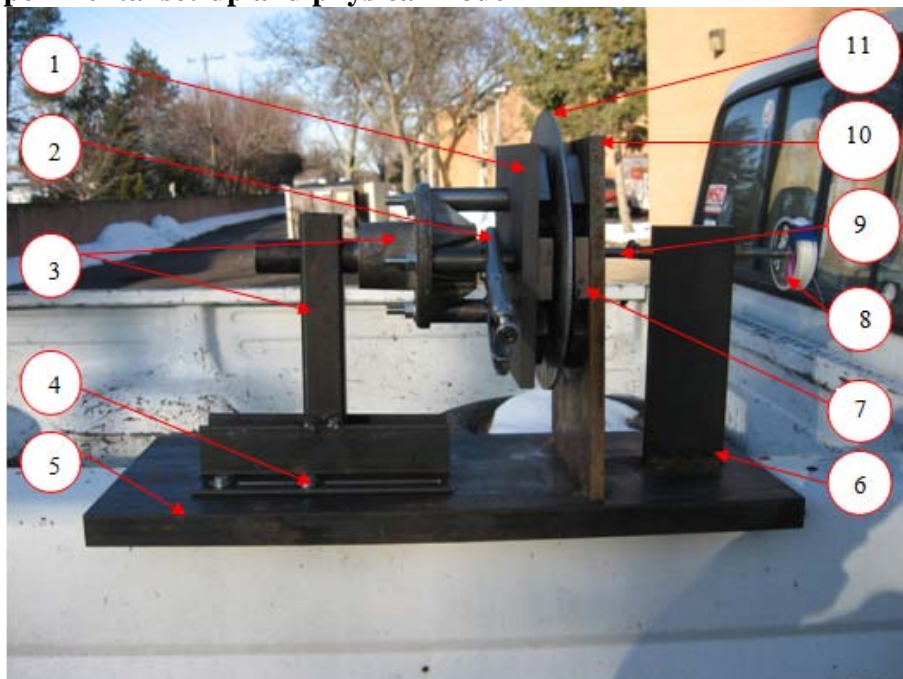
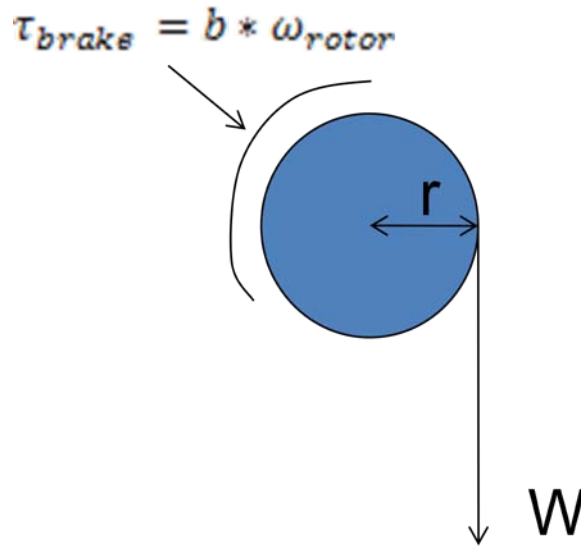


Table 2: Assembly part callout

Part #	Part Identification
1	Hub and Phasing Stator
2	Phase Tool
3	Hub Assembly
4	Hub Fastening Angle Bracket Assembly
5	Base Plate
6	Axel Stabilizer
7	Circular Arrangement of Magnets
8	Testing Spool
9	Axel
10	Right Stator
11	Aluminum Disk

Figure 4: Experimental FBD



Recall from Section 4.2 that the ECB can be modeled as a viscous damper. Equation 14 shows the governing equation for forced response of the ECB. In our experiment the rotor reached steady state before data was recorded ($\ddot{\theta} = 0$) yielding Equation 15 with all known parameters except the damping coefficient, b . Substituting measured quantities and rearranging yields Equation 17. Thus, b is determined experimentally for the ECB on (b_{on}) and ECB off (b_{off}) cases.

$$I\ddot{\theta} + b\dot{\theta} = Wr \quad \text{Eqn. (14)}$$

$$b\dot{\theta} = Wr \quad \text{Eqn. (15)}$$

$$\dot{\theta} = \frac{2\pi}{t} \quad \text{Eqn. (16)}$$

$$b = \frac{Wrt}{2\pi} \quad \text{Eqn. (17)}$$

6.1.2 Experiment procedure

A known weight was attached onto the testing spool. Usually a larger weight was used for on case and a smaller weight for off case to adjust the time period of falling. We marked a position on the rotor. After dropping the weight, we used a stopwatch to measure the time in which the rotor finished its second full revolution. The first full revolution was considered in transition state and the second full revolution was estimated in steady state. By following this procedure, we obtained enough data for the calculation of the damping coefficient. The computational method has already been discussed in the previous section. Three repeated tests were done for each setup. Tests were performed under different conditions, such as different air gap distances, different radius of magnets circle, etc.

7 CONCEPT GENERATIONS AND EVALUATION

The ECB has been decomposed into three functionally distinct components: stator, rotor, and mechanical structure. The most suitable concepts for each of these components are presented in this section. Each is evaluated using functional decomposition and the *PI* and an alpha prototype component is selected. Additional concepts can be seen in Appendix D.

7.1 Stator

This section pertains to concepts of magnetic array patterns on the ECB stators. The top five concepts are discussed here and the remainder are presented in Appendix D.

7.1.1 Concept Overviews

Concept 1: Magnets are placed on a circle and one stator rotates to phase magnets.

Pro

- Simple
- Stator form used in physical prototype

Con

- Low index of performance

Figure 5: Concept 1



Concept 2: Same as Concept 1 except magnets are stacked to increase magnetic field strength.

Pro

- Simple
- Potentially more torque for the same inertia as physical prototype

Con

- Potentially more torque in the off position
- Requires more magnets, thus more expensive

Figure 6: Concept 2



Concept 3: Magnets are placed horizontally on stator and rotated 180 degrees to phase.

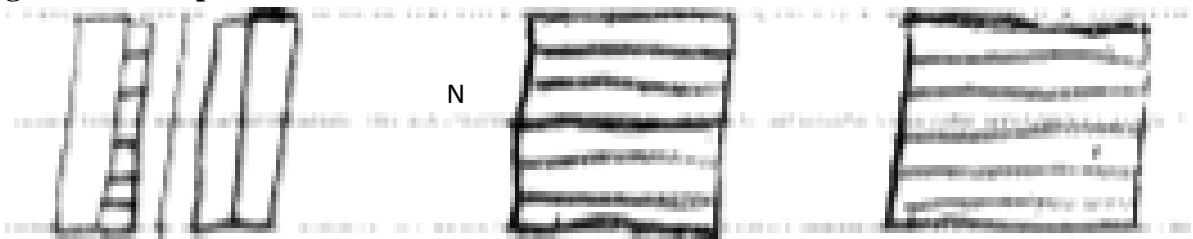
Pro

- Large flux density creating large torque

Con

- Large phase angle
- Requires more magnets, thus more expensive
-

Figure 7: Concept 3



Concept 4: Similar to Concept 2 except aluminum posts mounted on the stator capture stacked annular magnets.

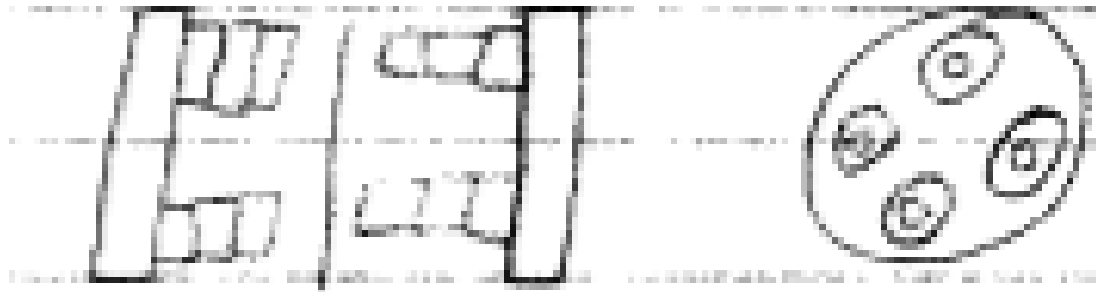
Pro

- Larger flux density creating larger torque
- Magnets are more stable

Con

- Requires more magnets, thus more expensive
- More manufacturing

Figure 8: Concept 4



Concept 6: Spring loaded magnets are placed in holes, machined in the stators, so that when the break is engaged the magnets pull themselves closer and when the break is off the magnets move apart.

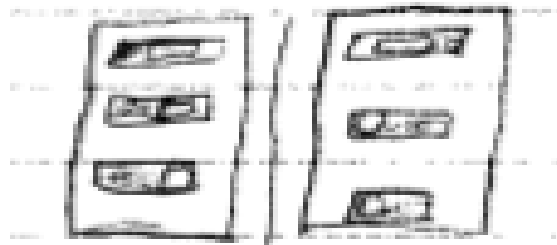
Pro

- Can get magnets very close to each other in the on position without paying a penalty in the off position

Con

- More manufacturing
- More complexity

Figure 9: Concept 6



7.1.2 Concept Evaluation

The advantage of concept 6 is that it allows the magnets to be very close the stator in the on position without paying a penalty in the off position. All of the other concepts try to increase the maximum torque by increasing the magnetic flux which has the disadvantage of increasing ECB torque in both the on and off phases. Therefore we think that concept 6 will give us the best balance between max torque in the on position and min torque in the off position.

Experimentation and analysis will be used to further examine the optimum magnetic array pattern.

7.2 Rotor

This section presents concepts of rotor geometry.

7.2.1 Concept Overviews

Concept 1: Single spoke rotor

Pro

- Lowest inertia
- Lowered ECB off torque

Con

- Rotating imbalance
- More machining
- Low rigidity
- Difficult to mount to axle – complex hub
- Only one concentric ring of magnets possible

Figure 10: Concept 1



Concept 2: Dual spoke rotor

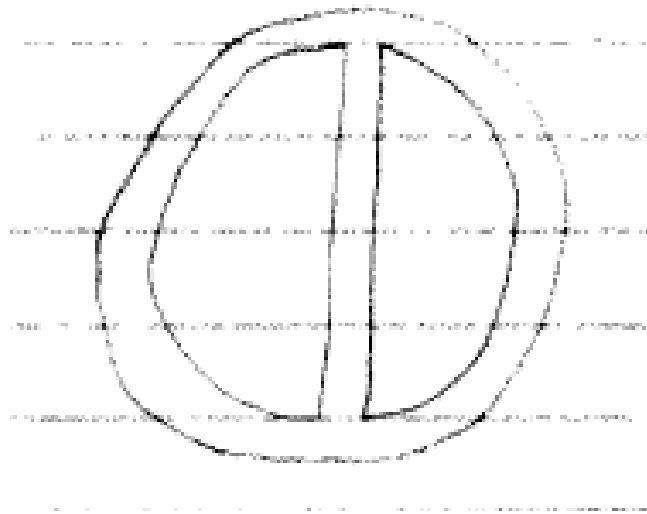
Pro

- Low inertia
- Lowered ECB off torque

Con

- More machining
- Low rigidity
- Difficult to mount to axle – complex hub
- Only one concentric ring of magnets possible

Figure 11: Concept 2



Concept 3: Three spoke rotor

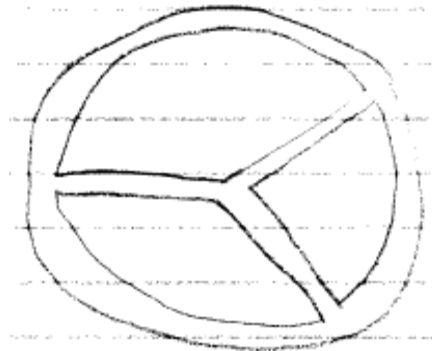
Pro

- Modest inertia
- Lowered ECB off torque

Con

- More machining
- Modest rigidity
- Only one concentric ring of magnets possible

Figure 12: Concept 3



Concept 4: Four spoke rotor

Pro

- Modest inertia
- Lowered ECB off torque

Con

- More machining
- Modest rigidity
- Only one concentric ring of magnets possible

Figure 13: Concept 4



Concept 5: Solid disk rotor

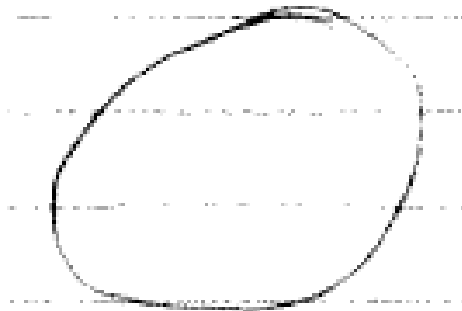
Pro

- Maximum rigidity
- Maximum surface area for eddy currents (can use multiple concentric rings)
- Simple shape

Con

- Maximum inertia (significant)

Figure 14: Concept 5



7.2.2 Concept Evaluation

Experimentation and analysis will be used to further examine the optimum rotor geometry.

7.3 Mechanical Structure

This section presents design concepts of the mechanical structure of the ECB.

7.3.1 Concept Overviews

Concept 1: One-side-closed package

We are using this package in the physical model. The idea is to physically restrain the freedom of the bottom side. One stator is welded on the base and the other stator is attached into a track, allowing one degree of freedom along the rotating shaft.

Pro

- It is easiest to build
- Component interchangeability

Con

- Great shear stresses are induced on the contact points (welding points), especially when magnets are placed in off-case, causing large repulsive forces against each stator
- Metal fatigue is a potential failure mode because it is subject to cycle loading between on and off cases
- Two stators are inclined in off-case

Concept 2: Multi-side-closed package

This design is similar to the first one, except we propose a mechanical closed-loop for structure. Top side is closed to form the closed-loop with the bottom side. It is optional whether to close left and right sides.

Pro

- It approximately reduces half of shear stresses on bottom contact points
- Stator inclination is eliminated

Con

- It is relatively difficult to build because we need to build another track on top
- It is not as adjustable or interchangeable
- Metal fatigue is still a potential failure mode
- Normal stresses or shear stresses are also existing on top contact point, depending on how we weld

Concept 3: Spring-connected stators

This design implements springs to stabilize one stator and still attach the other stator on the track. Figure 15 shows a sketch of this concept. The left stator is attached to the left fixed wall. Springs will not reduce stresses or dissipate potential energies. However, because of great repulsive forces existing in ECB off-case, the stator spacing air gap increases, which counteracts the repulsion. In addition, large air gap happens to be desirable to achieve optimal backdrivability.

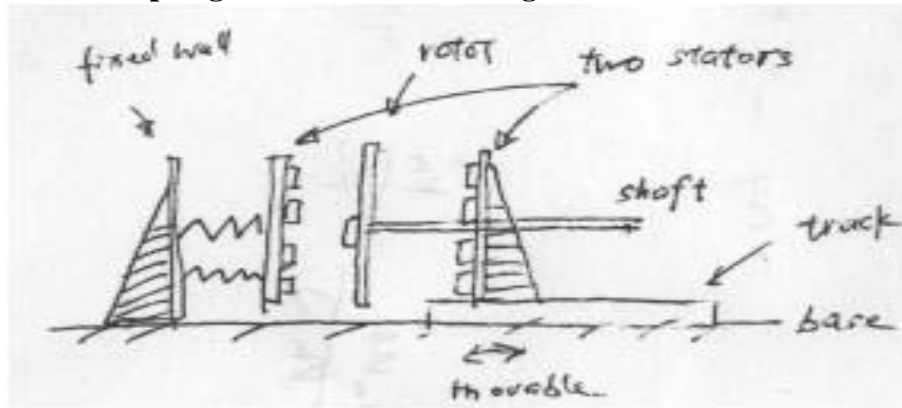
Pro

- Magnetic flux decreases in off-case, which gives good backdrivability
- Inclination is eliminated
- Reduces a large amount of stress on contact points

Con

- It is very difficult to build. The difficulties are finding the equilibrium position, locating springs and so on

Figure 15: Sketch of spring-connected stator design



7.3.2 Concept Evaluation

Currently concept one is being evaluated in the form of the physical prototype. Analysis on concept two will also be done because of the large magnitude of the forces structural rigidity is an important design requirement.

8 PARAMETER ANALYSES ALPHA DESIGN

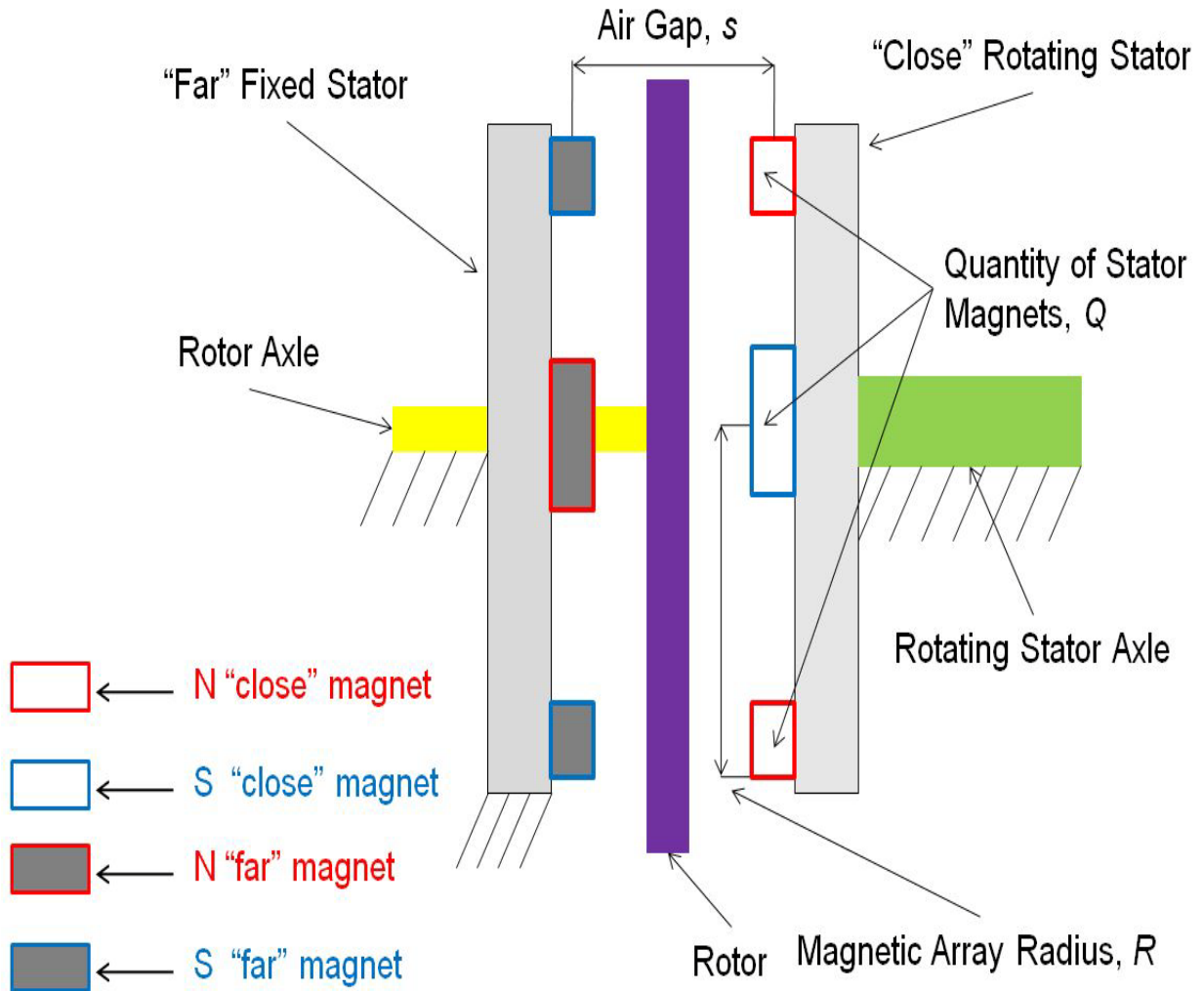
The dependence of the ECB damping coefficient (b) on stator air gap (s), magnetic array radius (R), quantity of stator magnets (Q), and stator phase angle (θ) were analyzed empirically. Analysis was performed on the physical prototype ECB (Figure 3) by the experimental procedure described in Section 7.1.1. It is reasonable to assume that any empirical trends present in the physical prototype ECB approximately represent “global” trends that will persist in the final ECB design. Therefore, this analysis will be used to inform the final design.

Further, analysis was performed numerically on stator air gap (s), and length between magnets (l) using *Vizimag* software [8]. Again, it is reasonable to assume that any trends present in the numerical analysis approximately represent “global” trends that will persist in the final ECB design. Therefore, this analysis will be used to inform the final design.

8.1 Definition of Parameters

This section clearly defines the ECB design parameters that have been analyzed. Specifically, the stator air gap, s is measured from the magnet center to magnet center. The magnet array radius, R is measured from the center of the stator to the inside of the magnet and the quantity of stator magnets, Q is a count of the magnets on one stator (Figure 16).

Figure 16: Definition of Stator Air Gap (s), Magnetic Array Radius (R), and Quantity of Stator Magnets (Q)

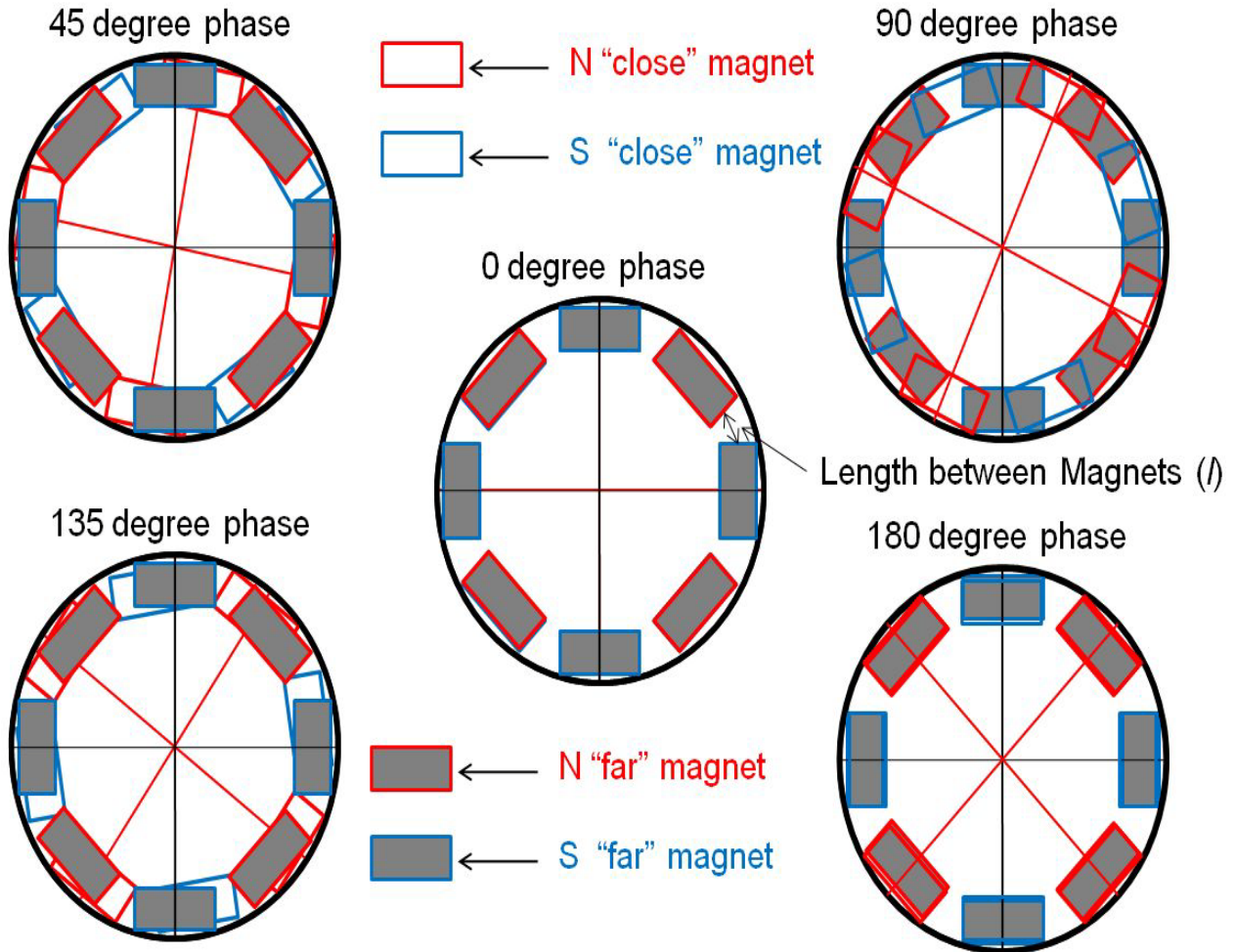


The stator phase angle is the measurement of the degree the ECB is ON. When the ECB is ON the stator magnet pairs are attracting and the phase is 0° . When ECB is OFF the stator magnet pairs are repelling and the phase is 180° . Phases in between these extremes are partially ON modes and increase from full ECB ON to full ECB OFF (Figure 17). The actual stator rotation angle, Φ is defined as a function of the quantity of stator magnets, Q as in equation 18.

$$\Phi = \frac{\theta}{Q} \quad \text{Eqn. (18)}$$

The length between magnets (l) is defined as the average distance between the end of the magnets as in Figure 17.

Figure 17: Definition of Stator Phase Angle (θ), and Length between Magnets (l)



8.2 Stator Air Gap

Values of parameters and damping coefficient results for this experimental set are presented in Table 3. The varied parameter is highlighted for clarity. The coefficient of damping of the ECB-ON decreases as the air gap increases (Figure 18). The physical prototype demonstrated good braking strength with air gaps up to 0.04 meters.

The built-in frictional damping of the physical prototype was determined by removing the stator magnets in order to eliminate any eddy current effects. This value was found to be small compared to the damping in the ECB-ON case, but significant in the ECB-OFF case. Further, frictional damping will be eliminated in the final design by use of roller bearings instead of plain bearings.

Figure 18: Damping Coefficient as a Function of Air Gap – ECB ON

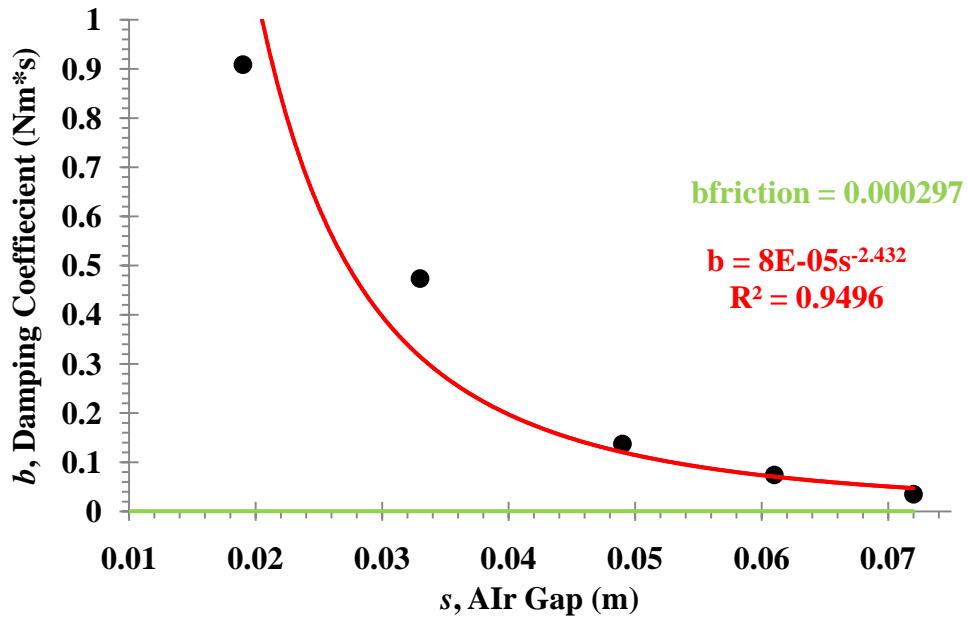


Table 3: Damping Coefficient as a Function of Air Gap – ECB ON

Quantity of				
Stator Magnets, Q	Magnetic Array Radius, R (m)	Phase Angle, θ (degrees)	Air Gap, s (m)	Weight, W (N)
8	0.089	0	0.019	4.89
8	0.089	0	0.033	4.89
8	0.089	0	0.049	4.89
8	0.089	0	0.061	4.89
8	0.089	0	0.072	4.89

Rotor Angular				
Moment Arm, r (m)	Time (s)	Velocity, ω (rad/s)	Torque, τ (Nm)	Damping coefficient, b (Nm*s)
0.04	29.19	0.22	0.1956	0.9087
0.04	15.21	0.41	0.1956	0.4735
0.04	4.41	1.42	0.1956	0.1373
0.04	2.38	2.64	0.1956	0.0741
0.04	1.12	5.61	0.1956	0.0349

Values of parameters and damping coefficient results for this experimental set are presented in Table 4. The varied parameter is highlighted for clarity. The coefficient of damping of the ECB-OFF decreases as the air gap increases (Figure 19). The ECB-OFF damping coefficient is an order of magnitude smaller than the ECB-ON case, which is desirable. Further, the physical

prototype demonstrated good backdriveability with air gaps greater than 0.04 meters. The ECB-OFF damping coefficient goes to zero when the frictional damping is subtracted.

Figure 19: Damping Coefficient as a Function of Air Gap – ECB OFF

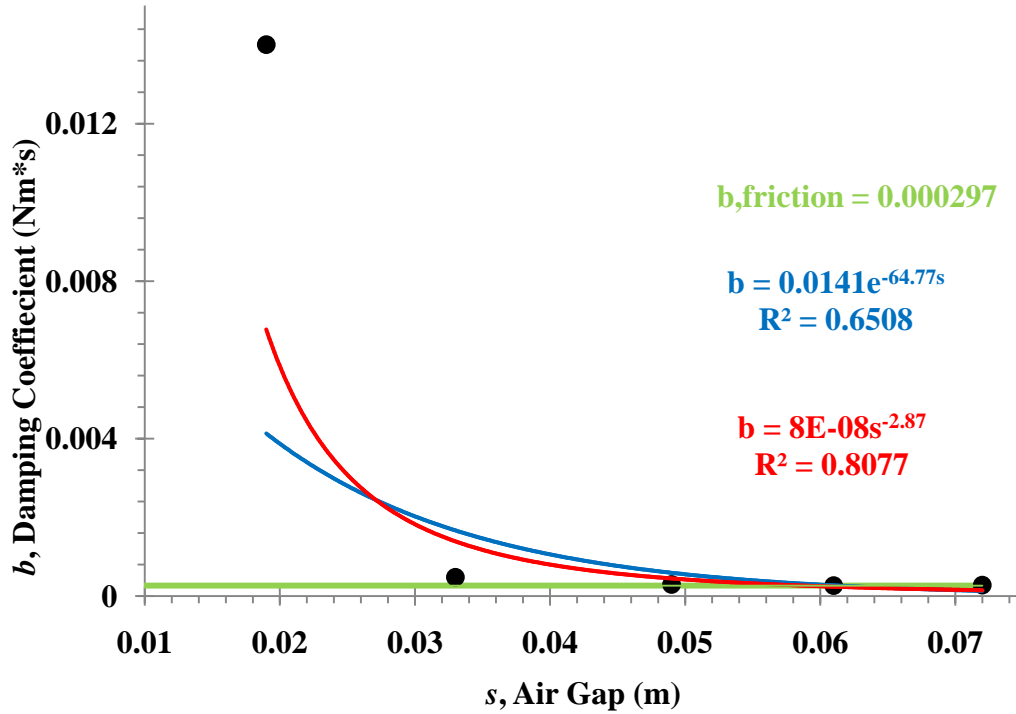


Table 4: Damping Coefficient as a Function of Air Gap – ECB OFF

Quantity of				
Stator Magnets, Q	Magnetic Array Radius, R (m)	Phase Angle, θ (degrees)	Air Gap, s (m)	Weight, W (N)
8	0.089	180	0.019	4.89
8	0.089	180	0.033	0.09
8	0.089	180	0.049	0.09
8	0.089	180	0.061	0.09
8	0.089	180	0.072	0.09
Moment Arm, r (m)	Time (s)	Rotor Angular Velocity, ω (rad/s)	Torque, τ (Nm)	Damping coefficient, b (Nm*s)
0.04	0.45	13.96	0.1956	0.0140
0.04	0.81	7.76	0.0037	0.0005
0.04	0.50	12.57	0.0037	0.0003
0.04	0.45	13.96	0.0037	0.0003
0.04	0.47	13.37	0.0037	0.0003

In order to inform the final design, the results of the ECB-ON and ECB-OFF case were combined. The effect of frictional damping was subtracted because it will be eliminated in the final design. Figure 20 shows that an air gap of approximately 0.0325 meters is optimal. The ECB-ON damping is significant while the ECB-OFF damping is virtually zero. Values of parameters and damping coefficient results for the experiment determining frictional damping are presented in Table 5.

Figure 20: Damping Coefficient as a Function of Air Gap – ECB ON and OFF

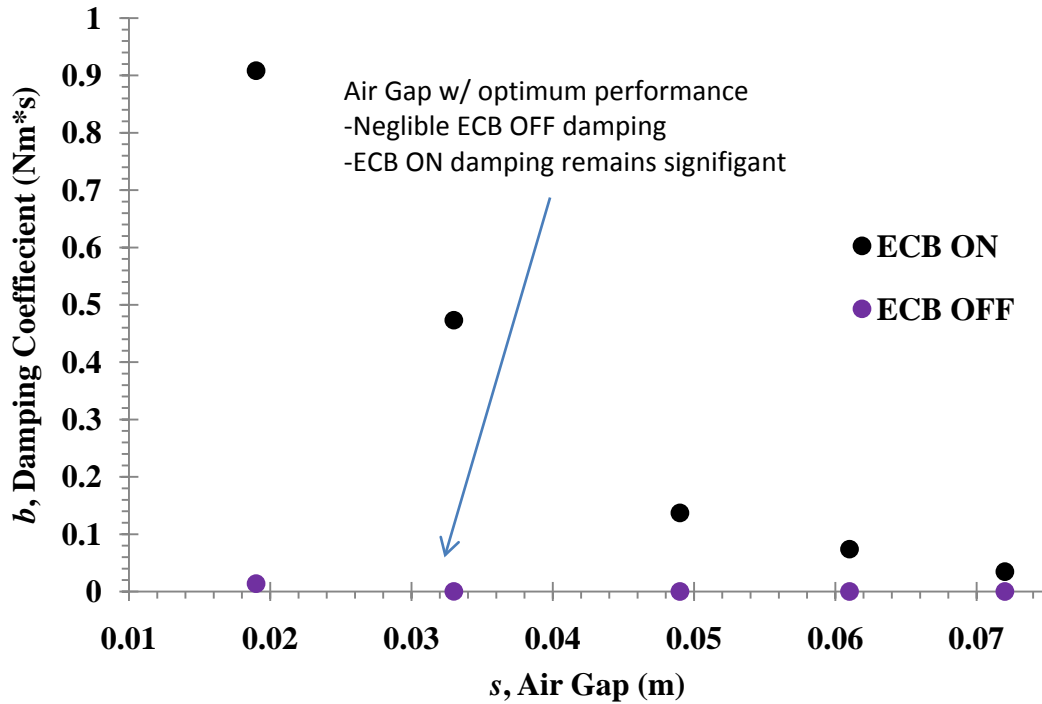


Table 5: Physical Prototype Frictional Damping

Quantity of				
Stator Magnets, Q	Magnetic Array Radius, R (m)	Phase Angle, θ (degrees)	Air Gap, s (m)	Weight, W (N)
-	0.089	Friction	0.019	0.09
Moment Arm, r (m)	Time (s)	Rotor Angular Velocity, ω (rad/s)	Torque, τ (Nm)	Damping coefficient, b (Nm*s)
0.04	0.45	13.96	0.0037	0.0003

8.3 Stator Phase Angle

Values of parameters and damping coefficient results for this experimental set are presented in Table 6. The varied parameter is highlighted for clarity. The coefficient of damping of the ECB decreases as the phase angle gap increases (Figure 21). The physical prototype demonstrated good braking strength with phase angles up to 45 degrees.

We had very little intuition on the functional dependence of the damping coefficient on the phase angle. The results presented in this section are not rigorous enough to claim a universal definition

of dependence. Therefore, the functional dependence would not be a suitable means of dynamically controlling ECM torque. An experiment would have to be designed in order to test and confirm our findings. Alternatively, future dynamic control of ECM torque would be better implemented via a torque sensing feedback control system.

Figure 21: Damping Coefficient as a Function of Stator Phase Angle – ECB ON

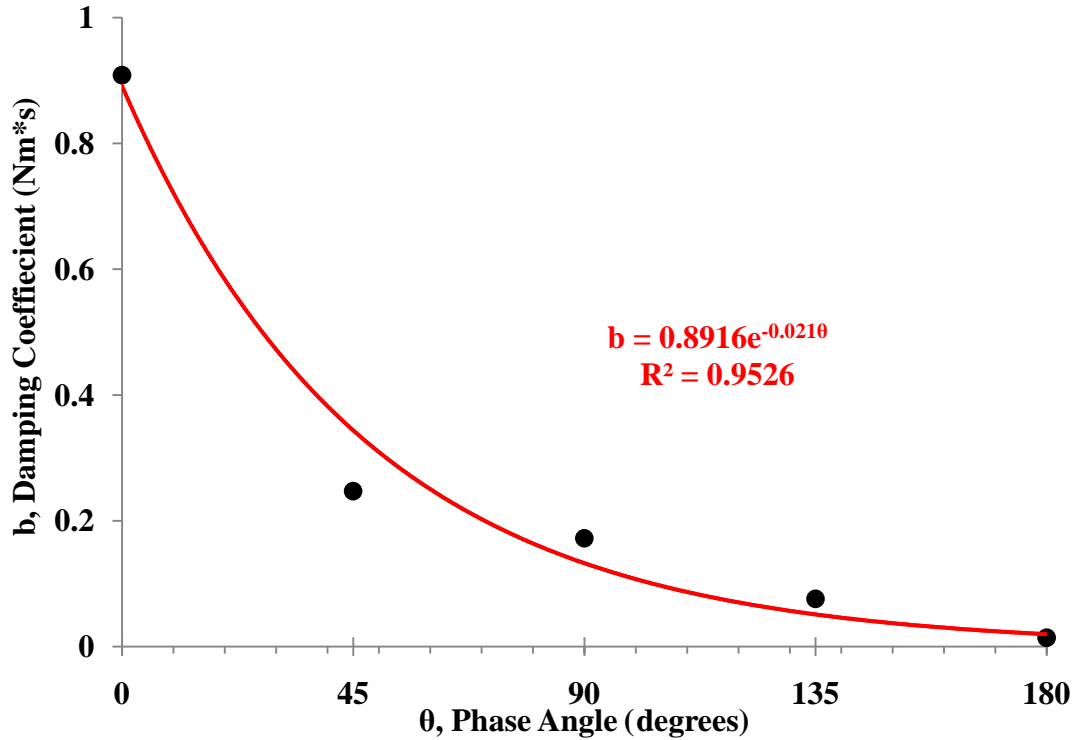


Table 6: Damping Coefficient as a Function of Stator Phase Angle – ECB ON

Quantity of				
Stator Magnets, Q	Magnetic Array Radius, R (m)	Phase Angle, θ (degrees)	Air Gap, s (m)	Weight, W (N)
8	0.089	0	0.019	4.89
8	0.089	45	0.019	4.89
8	0.089	90	0.019	4.89
8	0.089	135	0.019	4.89
8	0.089	180	0.019	4.89

Moment Arm, r (m)	Time (s)	Rotor Angular Velocity, ω (rad/s)	Torque, τ (Nm)	Damping coefficient, b (Nm*s)
0.04	29.19	0.22	0.1956	0.9087
0.04	7.94	0.79	0.1956	0.2472
0.04	5.53	1.14	0.1956	0.1722
0.04	2.44	2.58	0.1956	0.0760
0.04	0.45	13.96	0.1956	0.0140

8.4 Magnetic Array Radius

Values of parameters and damping coefficient results for this experimental set are presented in Table 7. The varied parameter is highlighted for clarity. The coefficient of damping of the ECB increases as the magnetic array radius increases (Figure 22). This result is expected because the magnetic array radius acts as a moment arm.

Figure 22: Damping Coefficient as a Function of Magnetic Array Radius – ECB ON

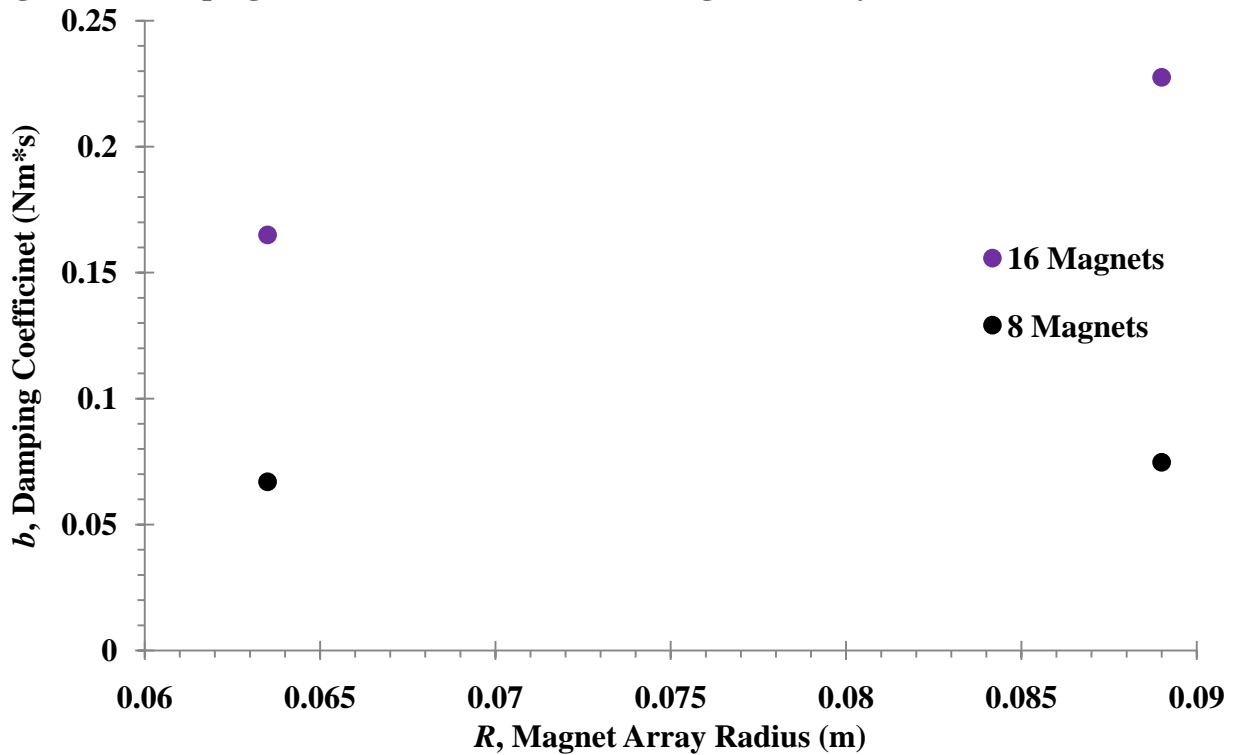


Table 7: Damping Coefficient as a Function of Magnetic Array Radius – ECB ON

Quantity of				
Stator Magnets, Q	Magnetic Array Radius, R (m)	Phase Angle, θ (degrees)	Air Gap, s (m)	Weight, W (N)
16	0.089	0	0.019	4.89
16	0.064	0	0.019	4.89
8	0.089	0	0.019	4.89
8	0.064	0	0.019	4.89
Moment Arm, r (m)	Time (s)	Rotor Angular Velocity, ω (rad/s)	Torque, τ (Nm)	Damping coefficient, b (Nm*s)
0.04	7.31	0.86	0.1956	0.2276
0.04	5.30	1.19	0.1956	0.1650
0.04	2.40	2.62	0.1956	0.0747
0.04	2.15	2.92	0.1956	0.0669

8.5 Quantity of Stator Magnets

Values of parameters and damping coefficient results for this experimental set are presented in Table 8. The varied parameter is highlighted for clarity. The coefficient of damping of the ECB increases as the quantity of stator magnets increases (Figure 23). This result is expected because increasing the quantity of magnets increases the amount of magnetic flux and the change of magnetic flux through the rotor.

Figure 23: Damping Coefficient as a Function of Quantity of Stator Magnets – ECB ON

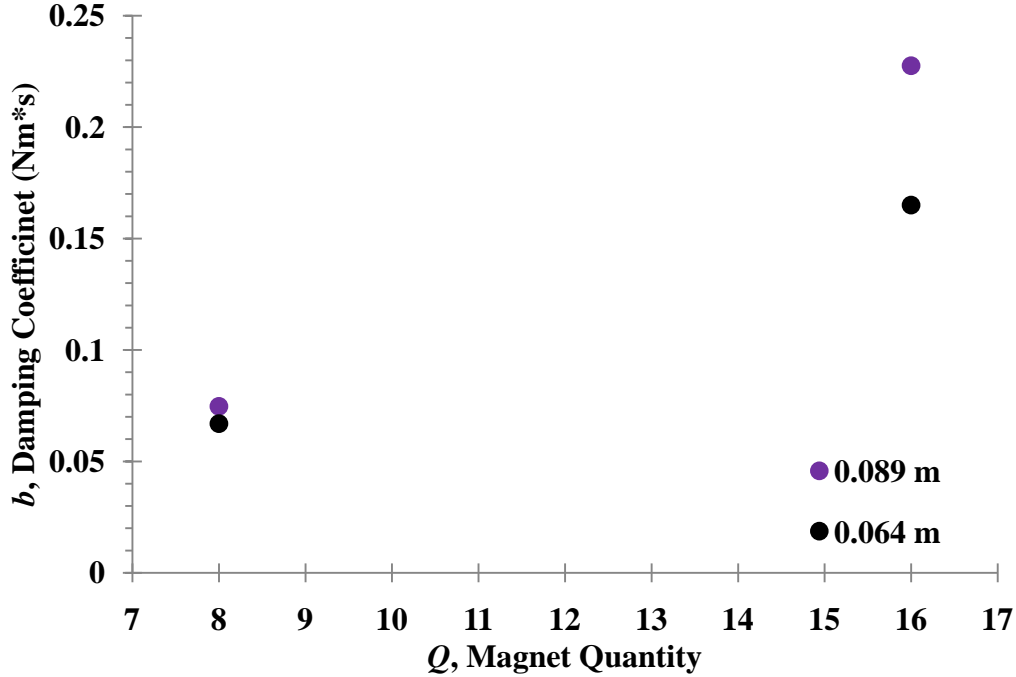


Table 8: Damping Coefficient as a Function of Quantity of Stator Magnets – ECB ON

Quantity of Stator Magnets, Q				
Magnets, Q	Magnetic Array Radius, R (m)	Phase Angle, θ (degrees)	Air Gap, s (m)	Weight, W (N)
16	0.089	0	0.019	4.89
8	0.089	0	0.019	4.89
16	0.064	0	0.019	4.89
8	0.064	0	0.019	4.89

Rotor Angular				
Moment Arm, r (m)	Time (s)	Velocity, ω (rad/s)	Torque, τ (Nm)	Damping coefficient, b (Nm*s)
0.04	7.31	0.86	0.1956	0.2276
0.04	2.40	2.62	0.1956	0.0747
0.04	5.30	1.19	0.1956	0.1650
0.04	2.15	2.92	0.1956	0.0669

8.6 Vizimag Analysis

We used *Vizimag* [8] to look at various magnetic array arrangements to see how they would affect the performance of the brake.

8.6.1 Procedure

To begin, a series of magnetic array arrangements were designed in *Vizimag* for parameter analyses. Plots of magnetic flux through the stator for each magnetic array arrangement were generated for both ECB-ON and ECB-OFF cases. Since, the performance of the ECB is related to the magnitude of magnetic flux and the amount of change in magnetic flux through the stator, a line integral of the plots was estimated in order to evaluate the ECB performance. This was done by taking the magnitude of flux and multiplying it by the number of cycles of the flux, as reported by *Vizimag*, through the stator.

Figure 24: Change in flux as the rotor moves between the stator

8.6.2 Magnet spacing

We tested the length between magnets (l) as in the three layouts in Figure 25, shown below. We found that there is an optimum length between magnets somewhere between the extremes of touching and two times a single magnets length.

Figure 25: Different lengths between magnets

Figure 26: Length between magnets has an optimum

8.6.3 Stator Spacing

The stator air gap was also evaluated numerically. We found that the optimum stator air gap is approximately two times the width of an individual magnet. The simulated results presented in this section agree and serve as confirmation of the empirical results discussed earlier.

Figure 27: Stator air gap

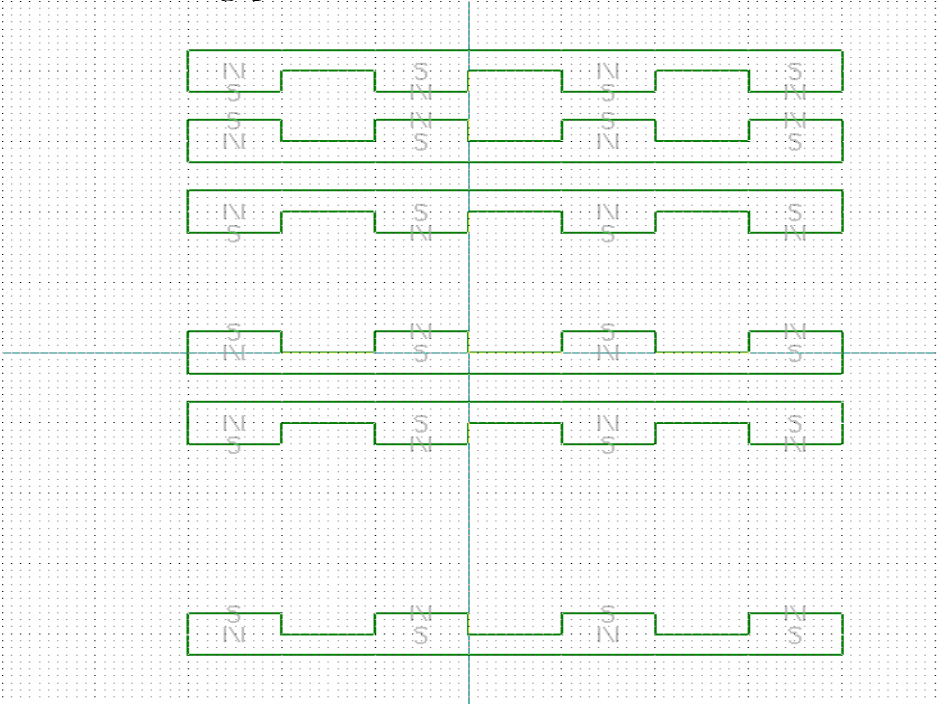
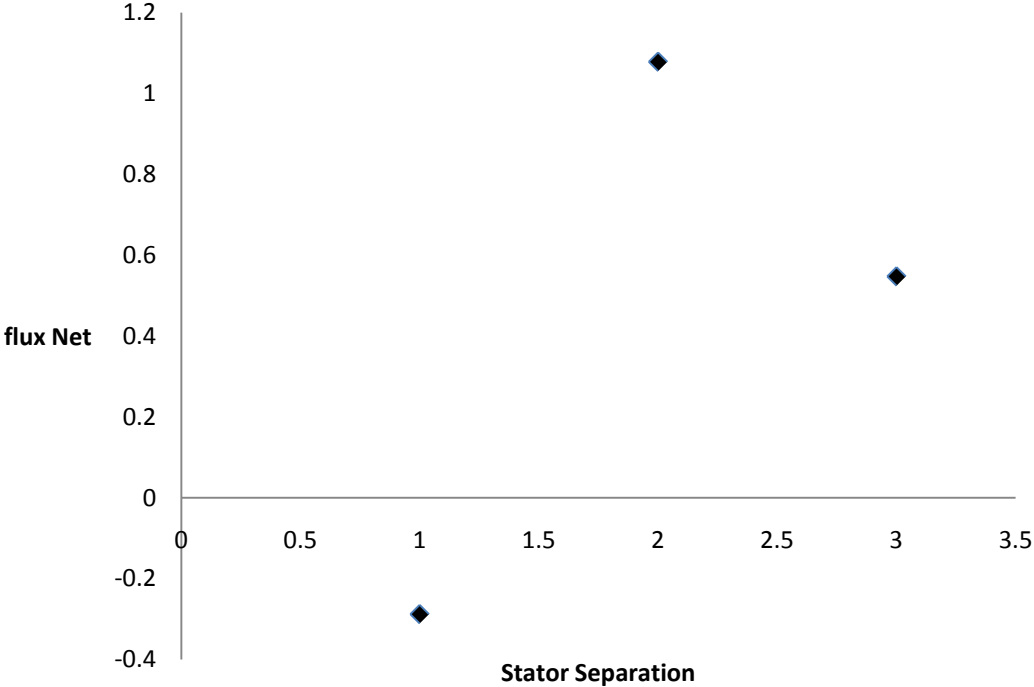


Figure 28: Force with different stator air gap



8.7 Summary of Material Selections

By use of Cambridge Engineering Selector (CES), we are able to search among all bulk materials for the best candidates according to our prescribed criteria or so-called material indices. We choose aluminum to be the material of the rotor because of high electric conductivity and low density, which may help us better achieve the prescribed engineering specifications. We choose steel to be the material of the stator because of high strength and low density. After calculating the environmental impact of the use of these two materials, we conclude that steel has more significant impacts, which is indicated by a higher EcoIndicator 99 “point value”. “Resources” is most likely to be important among all three damage meta-categories.

8.8 Summary of Manufacturing Process

By use of Cambridge Engineering Selector (CES), we are able to search among all manufacturing processes for the best candidates according to our prescribed criteria and a production quantity of 1000-2000 units. The stainless steel rotor is to be shaped by guillotine and have holes machined it via drilling. The aluminum rotor is to be shaped by parting o a lathe and have a center hole bored on a lathe.

9 SAFETY ANALYSES

In this section, we show the results of the safety analyses on the stresses at the welded joints. Further, we analyzed whether the magnets need to be secured to the stators or if friction is sufficient.

9.1 Open-Structure Housing

In this device there exists storage of potential energy due to the magnetic potential that is always present. Further, this potential changes direction depending on whether the ECB is ON or OFF. For example, the magnitude of repelling forces between each pair of magnets is approximately 30N when separated by 1 inch [9]. This given parameter is confirmed by observation of the physical prototype. When the physical prototype was OFF the fixed stator had a significant bending shape. Thus, we are motivated to perform thorough safety analyses of the ECB structure, especially at some significant stress concentration locations. The most dangerous location on the structure is identified to be the welded joints between the fixed stator and the base plate. Thus, we perform the stress analyses at this location and compare results with some material properties to check for failures, such as yielding or fatigue.

We have made three assumptions during the analyses:

- i. We solve the problem in two dimensions, neglecting the bending effect associated with the depth of the stator. Thus converting the problem into a simple beam analyses. By assuming this, we overestimate the maximum stress at the joints, which makes our analysis conservative.
- ii. The phasing stator is considered to be rigid. This assumption is confirmed by observation.
- iii. Stresses only concentrate at the two welded joints, not over the entire cross-sectional area of the stator. We validate this assumption by comparing the calculated deflection at the top end of the stator with the physical measurement.

Figure 29: Free body diagram of the stator in the open-structure housing

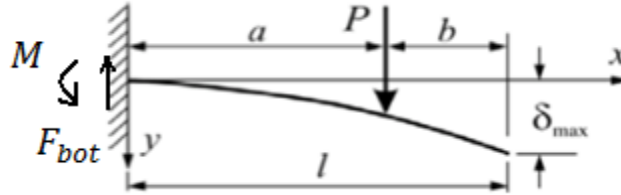


Figure 29 shows the free body diagram of the beam analyses problem. The equations of force balance and moment balance are shown:

$$F_{bot} - P = 0 \quad \text{Eqn. (19)}$$

$$M = P \cdot a \quad \text{Eqn. (20)}$$

There are two unknowns in the equations: the shear force F_{bot} and the bending moment M . The net repelling force P is estimated to be 30 N per pair of magnets, multiplying 8 pairs according to the manufactures web site[9]. Thus, the shear force F_{bot} is found to be 240 N and the bending moment M is found to be 48 N·m. The resulting shear stress τ and normal stress σ are found to be 0.7 MPa and 71.2 MPa using Equations 21 and 22.

$$\tau = \frac{F_{bot}}{A} \quad \text{Eqn. (21)}$$

$$\sigma = \frac{M \cdot y}{I} \quad \text{Eqn. (22)}$$

Here A is the cross-sectional area of the welded region, y is the distance from the edge to the neutral axis of the stator and I is the second moment of inertia. The deflection δ is calculated using Equation 23 and found to be 5.4 mm, which matches the physical measurement well.

$$\delta = \frac{Pa^2}{6EI} (3l - a) \quad \text{Eqn. (23)}$$

The weld filler material used is steel, of which the yielding strength is several hundred MPa. Therefore, a large safety factor against yielding exists. Fatigue, however, is a potential failure mode when the stator is subject to cyclic loading (cycling between ECB-ON and ECB-OFF). Further, analyses of this failure mode would have to be performed if the open-structure housing is selected because cycling is likely.

9.2 Closed-Structure Housing

Although, we have proved the open-structure housing relatively safe, we still want to make a mechanical close loop in order to eliminate deflections, thus greatly reducing fatigue. Figure 28 shows both housing options. Here, we show the safety analyses done for this closed-housing option and the significance of the stress reduction at the welded joint. However, the closed-structure is a much more complicated design analytically because there are three unknown loads existing simultaneously in the system, a bending moment M and a shear force F_{bot} at the bottom and a shear force F_{top} at the top. We can only take advantage of a so-called ‘energy method’ to deal with this statically indeterminate problem, in which we have to assume there is no

deformation at the top joints. This assumption can be validated after solving for the stress built at the top. If the stress is shown to be small, our assumption is then a reasonable one. Figure 31 shows the free body diagram of closed-structure option.

Figure 30: Two housing options analyzed in this section. (Dashed lines and shaded regions represent the ceiling closing the mechanical loop)

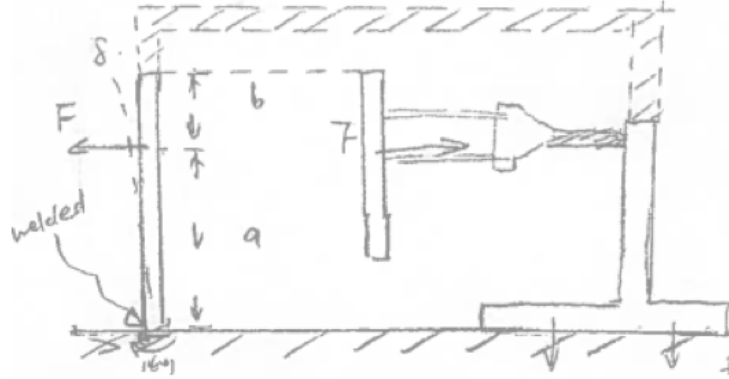
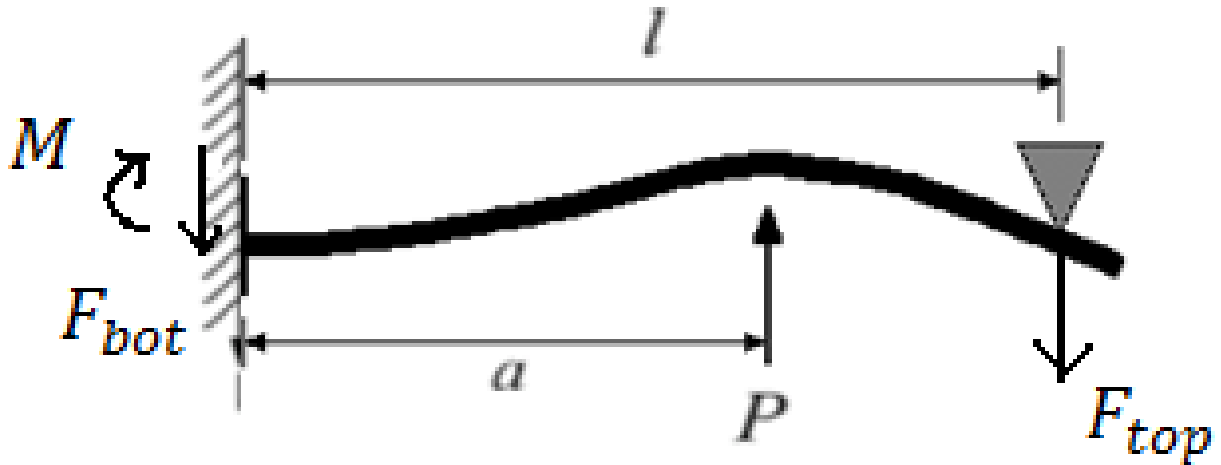


Figure 31: Free body diagram of the stator in the closed-structure housing



The equations of force balance and moment balance are shown:

$$F_{bot} + F_{top} - P = 0 \quad \text{Eqn. (24)}$$

$$M = P \cdot a - F_{top} \cdot l \quad \text{Eqn. (25)}$$

We equalize the deflection at the top of the fixed stator, v and the derivative of total energy of the system, U with respect to the force at that position F_{top} , shown in equation 26.

$$v = \frac{dU}{dF_{top}} = \int_0^l \frac{M(x)}{EI} \cdot \frac{dM(x)}{dF_{top}} dx \quad \text{Eqn. (26)}$$

After a series of algebraic operations, we obtain all unknown loads: F_{top} to be 28.7 N, F_{bot} to be 211.3 N and M to be 40.0 Nm. The resulting shear stress and normal stress at the bottom joints

are found to be 0.65 MPa and 58.4 MPa, respectively. In conclusion, the addition of a top closing structural member reduces approximately 20 percent of stresses. While the reduction in the magnitude of stresses may not be significant, the elimination of the deflections at the top end of the stator proves significant in its reduction of fatigue failure modes. The small magnitude of the force at the top of the stator validates our assumption that the top doesn't undergo large deformations.

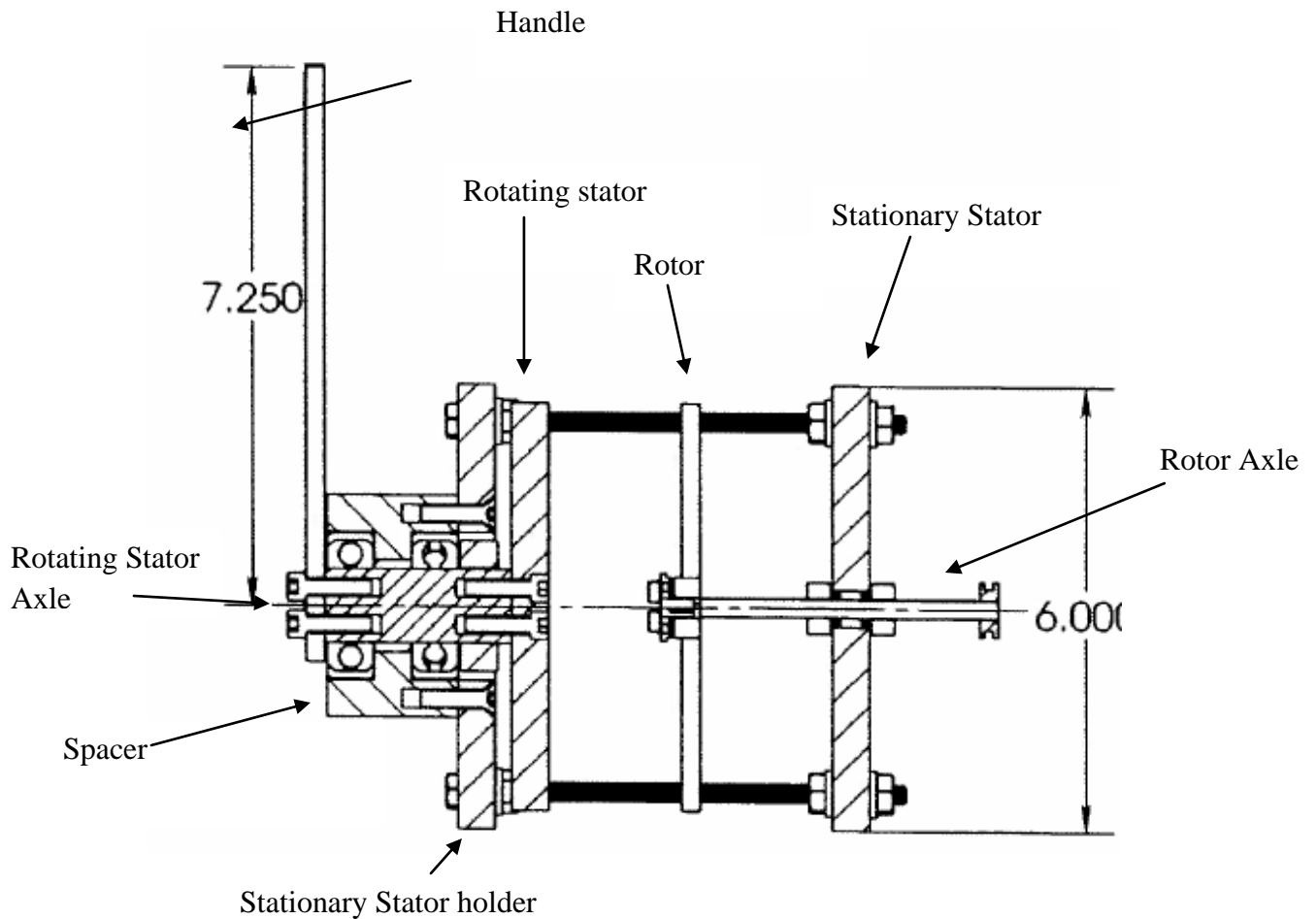
9.3 Friction

A calculator on the magnet manufacturer's web site [9] in order to calculate the force between the steel backing plate and the magnet which was found to be 77.7 lb. We were then able to calculate the maximum torque that we could apply to the brake by multiplying the force by the coefficient of friction (0.8), the number of magnets(16) and the moment arm (3 inch) and found the maximum torque to be about 3000 inch lbs. Thus, since this exceeds the operating range of the ECB it will not be necessary to affix mechanically affix the magnets to the stator.

10 FINAL DESIGN

We decided to go with a design that supports the forces between the magnets with four corner supports. We went with this design because it does not produce moments on the support components like our alpha design does. We did not go with a center supported design because we thought that there would be significant friction in the bearings supporting the rotating stator. We also decided to make the final design smaller than our alpha prototype so that we could use smaller magnets and make the device easier to experiment with. We added a handle and a clamp so that it is easier to phase the magnets. A problem with our alpha prototype was that it was difficult to adjust the spacing between the stators. We solved this problem by using nuts on a threaded rod instead of allowing one of the stators to slide as we did in previous designs. Also, all bolts on the face of the stator are counter bored so that magnets can be located anywhere on the face.

Figure 32: Final design



11 FABRICATION PLAN

The fabrication plan includes plans for manufacturing and assembly. The manufacturing plan completely analyzes the speeds, feeds and tooling procedures for each piece the team made and the assembly section explains the procedures to assemble our model in the appropriate order.

11.1 Manufacturing Plan

This section summarizes the specified manufacturing tooling procedures.

11.1.1 Handle

Manufacturing processes are outlined for the handle in Table 9.

Table 9: Handle Manufacturing Processes

Process	Machine	Tool	Speed
Drill through holes	Mill	HSS 1/4” Drill	1750 RPM
Drill through holes	Mill	HSS 1/4” Drill	3800 RPM

11.1.2 Stator Holder

Manufacturing processes are outlined for the stator holder in Table 10.

Table 10: Stator Holder Manufacturing Processes

Process	Machine	Tool	Speed
Drill “interior” through holes	Mill	HSS 1/4” Drill	1750 RPM
Counter bore holes	Mill	HSS End Mill 2 Flute – 3/8” 1/4” Depth	500 RPM
Drill “exterior” through holes	Mill	HSS 1/4” Drill	1900 RPM
Drill center hole	Lathe	HSS 2” drill	1900 RPM

11.1.3 Rotating Stator

Manufacturing processes are outlined for the rotating stator in Table 11.

Table 11: Rotating Stator Manufacturing Processes

Process	Machine	Tool	Speed
C	Mill	HSS 1/4” Drill	760 RPM
Counter bore holes	Mill	HSS End Mill 2 Flute – 3/8” 1/4” Depth	500 RPM
Drill through holes	Mill	HSS 1/4” Drill	1530 RPM

11.1.4 Rotating Stator Axle

Manufacturing processes are outlined for the rotating stator axle in Table 12.

Table 12: Rotating Stator Axle Manufacturing Processes

<u>Process</u>	<u>Machine</u>	<u>Tool</u>	<u>Speed</u>
Drill holes -Face A	Mill	HSS 1/4" Drill	760 RPM
Drill holes -Face A	Mill	HSS 1/8" Drill – Long Length	1500 RPM
Drill holes -Face B	Mill	HSS 1/4" Drill	760 RPM
Drill holes -Face B	Mill	HSS 1/8" Drill – Long Length	1500 RPM

11.1.5 Rotors

Manufacturing processes are outlined for the rotor (three) in Table 13.

Table 13: Rotor Manufacturing Processes

<u>Process</u>	<u>Machine</u>	<u>Tool</u>	<u>Speed</u>
Bore center hole	Lathe	HSS 0.900" Bore	2500 RPM

11.1.6 Spacer

Manufacturing processes are outlined for the spacer in Table 14.

Table 14: Spacer Manufacturing Processes

<u>Process</u>	<u>Machine</u>	<u>Tool</u>	<u>Speed</u>
Drill through holes	Mill	HSS #7 Drill -1" deep	1750 RPM
Tap	Bench top fixture	1/4" – 20 tap	-
Bore center through hole	Lathe	HSS 1" Bore	1200 RPM
Bore center hole - face A	Lathe	HSS 1 31/32" Bore	750 RPM
Bore center hole - face A	Lathe	HSS 1 31/32" Bore	750 RPM

11.1.7 Spacer for Rotor Plate

Manufacturing processes are outlined for the spacer for the rotor plate in Table 15.

Table 15: Spacer for Rotor Plate Manufacturing Processes

Process	Machine	Tool	Speed
Drill 4 perimeter holes	Mill	HSS #7 Drill -1" Deep	1750 RPM
Drill Center through hole	Mill	HSS 1/2" Drill	760 RPM

11.1.8 Stationary Stator

Manufacturing processes are outlined for the stationary stator in Table 16.

Table 16: Stationary Stator Manufacturing Processes

Process	Machine	Tool	Speed
Drill "interior" through holes	Mill	HSS 1/4" Drill	1750 RPM
Bore center hole	Lathe	HSS 1 31/32" Bore	750 RPM
Counter bore holes	Mill	HSS End Mill 2 Flute – 3/8" 1/4" Depth	500 RPM
Drill through holes	Mill	HSS 1/4" Drill	760 RPM
Drill center through hole	Mill	HSS Center Cut End Mill 2 Flute - 3/4"	400 RPM

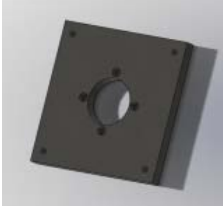




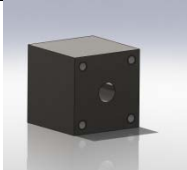
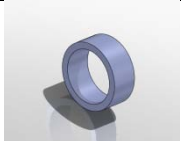
11.2 Assembly

All of the assembly instructions below represent step-by-step instructions for the construction of the prototype. There are multiple subassemblies and a final assembly. Subassemblies include: the handle-axle assembly, the handle-phasing plate assembly, the stator holder-spacer assembly and the stationary stator-rotor spacer assembly. Table 17 lists all of the tools, parts and quantity for one assembly of the ECB.

11.2.1 Sub-assemblies

This section includes a list of the sub-assemblies for construction of the beta prototype for our final ECB design.

Table 17: Package list of parts for assembly by category

Stators		
	Part Name	Quantity
	Stator Holder	1
	Stationary Stator	1
	Phasing Stator	1
Rotors		
	Part Name	Quantity
	Rotor	3 (Interchangeable sizes)
Spacers		
	Part Name	Quantity
	Phasor Spacer	1
	Rotor Spacer	1
	Bushing	1

		Spacer Washers	2
Shaft Collars			
		Part Name	Quantity
		Large Shaft Collar	1
		Small Shaft Collar for Rotor	2
Axles			
		Part Name	Quantity
		Main Axle	1
		Phasor Axle	1
Bearings			
		Part Name	Quantity
		Thrust Bearing	2
		Small Flange Bearing	2
Bolts			
		Part Name	Quantity
	Axle Bolts	2	
	Handle Bolts	2	
	Spacer Bolts	4	
	Stationary	4	




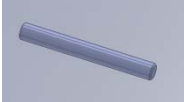
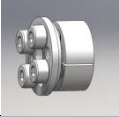
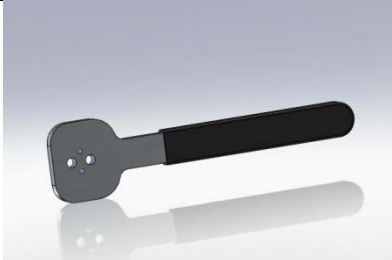
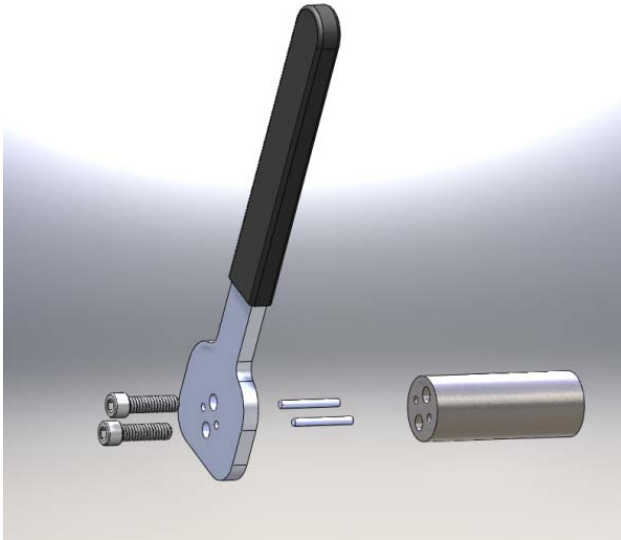
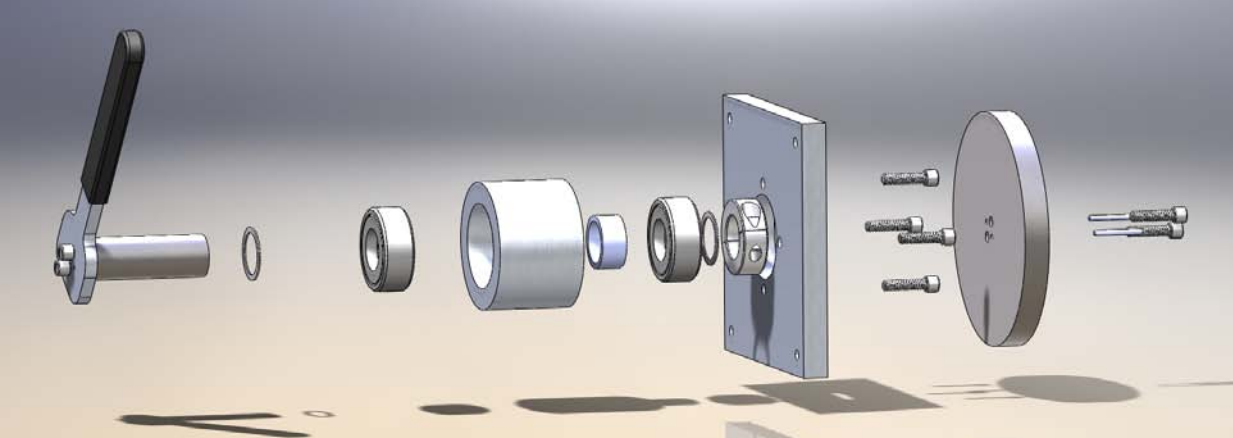
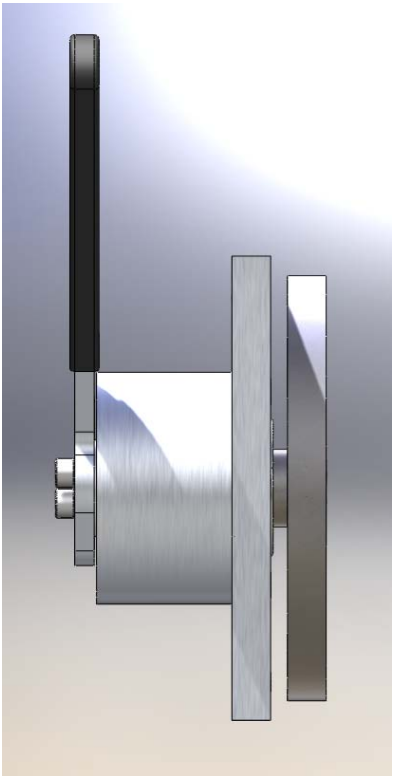
	Stator Bolts 6" Length 1/4" – 20 UNC Hex Bolt	4
Nuts		
	Part Name 1/4" – 20 UNC Hex Nut	Quantity 12
Miscellaneous		
	Part Name Pulley	Quantity 1
	Part Name Dowel Pin	Quantity 4
	Part Name Keyless Bushing	Quantity 1
	Part Name Handle with Custom Grip Manufactured to Hand	Quantity 1

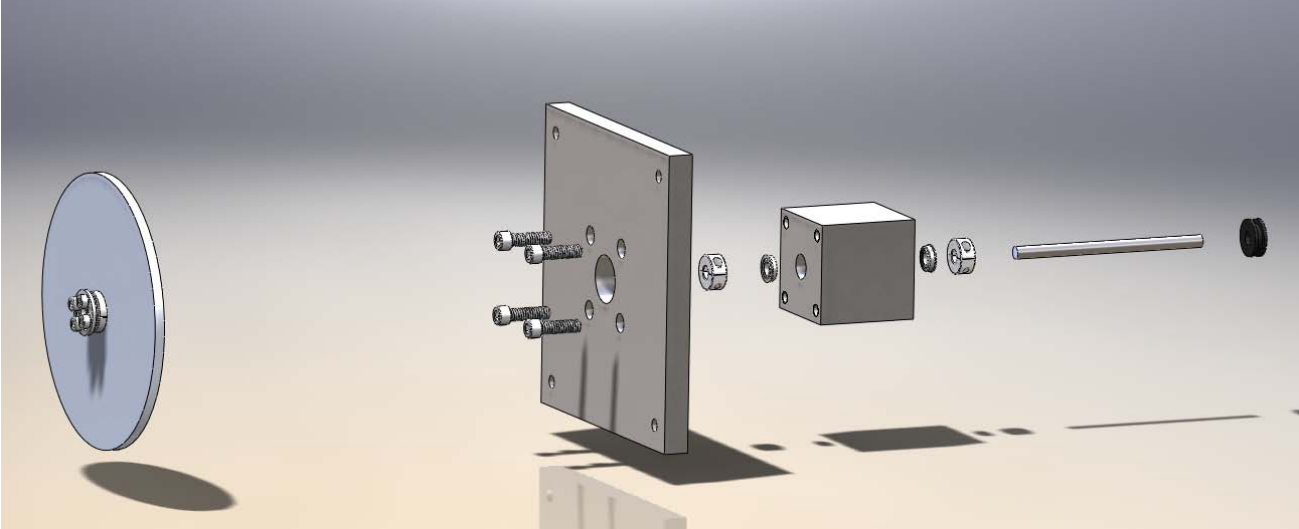
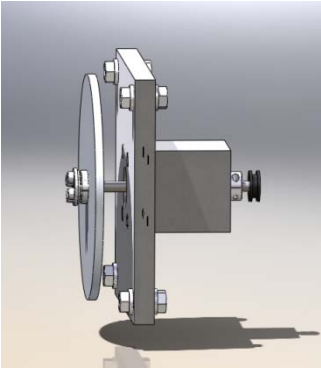
Table 18: A list of Sub-assemblies.

Phasing Assembly (left half by drawings)			
Handle-Axle			
	Tools Needed	Parts	Assembly
	<p>Allen Wrench</p> <p>Soft Metal Mallet</p>	<p>Custom Grip Handle</p> <p>Handle Bolts (2)</p> <p>Dowel Pins (2)</p> <p>Phasor Axle (1)</p>	<ol style="list-style-type: none"> 1. Check to make sure all of the holes line up from the handle to the axle (you may use the holes of the dowel pins until installing them to align). 2. Use the allen wrench to tighten the bolts loosely until face of the Phasor Axle is flush with Handle face. 3. Remove any alignment tools and use the Soft metal hammer to drive the dowels into the smaller holes until the dowel is flush with the handle face. 4. Finish tightening the bolts with allen wrench until snug.
Handle-Phasing Plate			
			

	Tools Needed	Parts	Assembly
	<p>—” Allen Wrench</p> <p>Soft Metal Mallet</p> <p>Chisel or large dowel</p>	<p>Handle-Axle Assembly (1)</p> <p>Washer (2)</p> <p>Thrust Bearing (2)</p> <p>Bushing (1)</p> <p>Spacer (1)</p> <p>Larger Shaft Collar (1)</p> <p>Axle Bolts (2)</p> <p>Spacer Bolts (4)</p> <p>Dowel Pins (2)</p> <p>Stator Holder (1)</p> <p>Phasing Stator Plate (1)</p>	<ol style="list-style-type: none"> 1. Slide the washer onto the axle on the Handle-Axle assembly. 2. Fit the thrust bearing in the spacer with the soft metal mallet and slide them onto the axle. 3. Use a chisel or a large dowel to pound the bushing in for a tight fit. 4. Fit the second bearing the same as in 2 with the metal mallet working around the edges so not to damage the axle. 5. Insert the second bearing around the axle and secure the second shaft collar using the Allen wrench. 6. Push through the Stator Holder and align holes with spacer holes. 7. Use Allen set to tighten the bolts alternating in a circular motion for about every .125” thread turned. 8. Check to make sure your product spins and align the holes on the phasing stator plate. 9. Use hammer to insert dowels into

			<p>the phasing plate and then through to the axle.</p> <p>10. Finally, fasten the axle bolts into the axle from the Phasing Stator Plate.</p> <p>11. Check that all of the plate faces are parallel to ensure a precise experiment.</p>
--	--	--	-------------------------------------------------------------------------------------------------------------------------------------------------------------------------------------------------------------------------------------------------------

Rotor and Disk Assembly (right half by drawings)

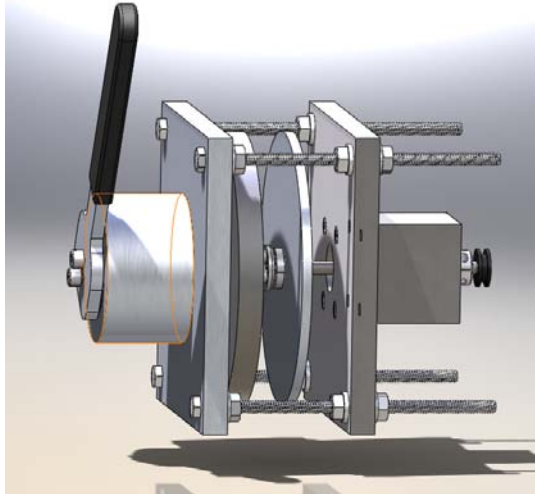
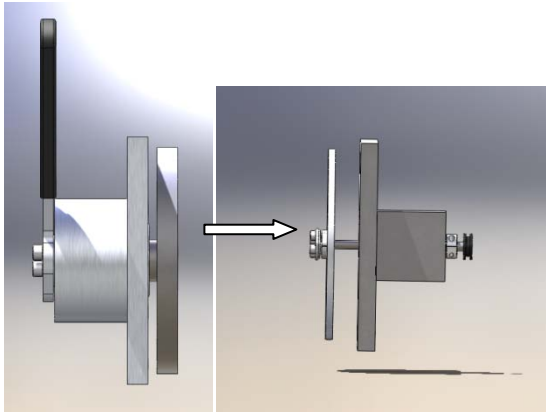
Stationary stator-rotor spacer	Tools Needed	Parts	Assembly
			
	<p>Rubber Mallet</p> <p>—” Allen Wrench</p> <p>—” Crescent Wrench</p>	<p>Keyless Bushing (1)</p> <p>Rotor (3 options)</p> <p>Stationary Bolts (4)</p> <p>Stationary Stator (1)</p> <p>Small Shaft Collar (2)</p>	<ol style="list-style-type: none"> 1. Use rubber mallet to press fit the pulley to the shaft. 2. Fasten the four spacer bolts to the spacer tightening different bolts every .125” thread length. 3. Slide the shaft through the through one shaft collar, then a flange bearing, then the spacer (flanges always face away from spacer) and back through another flange bearing and

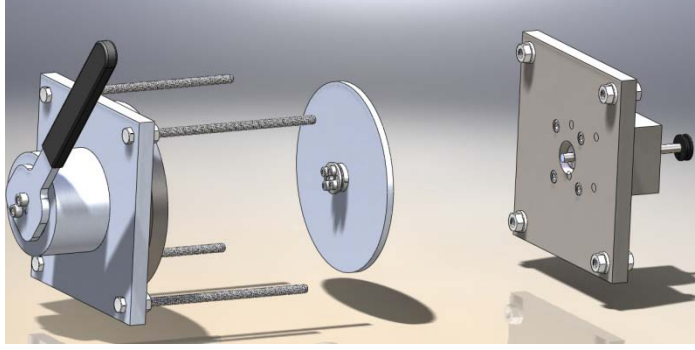
	<p>Flange Bearings (2)</p> <p>Spacer for Rotor (1)</p> <p>Main Shaft Axle (1)</p> <p>Pulley with string (1)</p>	<p>shaft collar. DO NOT TIGHTEN ANYTHING UNTIL YOU'VE POSITIONED EVERYTHING CORRECTLY.</p> <p>4. This is a good time to place your magnetic arrangement for this plate because of the flexibility of the system. Be careful because the magnets are strong enough to break themselves if near another magnet. After this is achieved and spacing is found, mark the shaft collar nearest the rotor, shift the shaft down and tighten it in the appropriate place and restore it back to its ideal position.</p> <p>5. Once everything is in place, tighten the keyless bushing around the shaft and rotor by attaching the rotor to keyless bushing by tightening its bolts with an Allen wrench while the shaft is flush with the edge of the keyless bushing.</p> <p>6. Finally, fasten the shaft collar on the pulley side while flush with the bearing with an Allen wrench to prevent movement.</p>
--	-----------------------------------------------------------------------------------------------------------------	-------------------------------------------------------------------------------------------------------------------------------------------------------------------------------------------------------------------------------------------------------------------------------------------------------------------------------------------------------------------------------------------------------------------------------------------------------------------------------------------------------------------------------------------------------------------------------------------------------------------------------------------------------------------------------------------------------------------------------------------------------------------------------------------------------------------------------------------------------------------------------------------------------------------------------

11.2.2 Full Assembly

This section includes the assembly of the two halves of the project mentioned in the table above. This is the assembly of our final beta prototype design.

Table 19: Full assembly

Beta Prototype Final Design Assembly			
			
	Tools Needed	Parts	Assembly
	<p>—” Crescent Wrench</p>	<p>Left Assembly (1)</p> <p>Right Assembly (1)</p> <p>6” Stator Bolts (4)</p> <p>Nuts (12)</p>	<ol style="list-style-type: none"> 1. Place all 4 bolts loosely through the left stator plate with the hex head flush with the plate’s face. 2. Tighten 4 of these nuts to the right face of this plate (look at the figure above). 3. Evenly spaced from the end of the bolt, place 4 more nuts about 2 inches down the bolt shaft from their ends. 4. Rest plate with magnets and right assembly attached against these nuts and put the last 4 nuts down the shaft to the back of the

			<p>plate.</p> <ol style="list-style-type: none"> 5. Place the magnets on the left plate either carefully before step 3 or wear gloves and do it now. 6. Reposition the plates to the testing distance by tightening the nuts on the right stator.
-----------------------------------------------------------------------------------	--	--	---------------------------------------------------------------------------------------------------------------------------------------------------------------------------------------------------------------------------------------------------------------------------

12 VALIDATION APPROACH

In this section, we present the validation approach, in which we demonstrate the degree to which the prescribed engineering specifications have been met. We are able to test for all the engineering specifications as discussed in Section 3.2 in details: torques generated in both on and off cases and the inertia of the rotor. Instead of reporting measurements of these specifications individually, we condense them in the performance index of our final design, and compare it with those of existing electric motors available in the market.

12.1 Experimental setup, procedure and measurements

The experimental setup, procedure and measurements are the same as what we have done and presented in Section 7.1. These approaches have been proved to be practical and reasonable physically. The only difference is that now we conduct tests on our final prototype, instead of the first physical prototype.

12.2 Validation results

Performance indexes are calculated based on the use of a reference angular velocity 2000 rpm and a reference angular acceleration 21 rad/s^2 (which means it takes 5 seconds to reach the reference velocity). Figure 33 shows the functional relationships between the performance indexes, rotor thicknesses and air gap distances. It's very obvious that the performance index decreases as the rotor thickness increases. The linearity cannot be determined so far. The change in performance index caused by different air gap distances is not significant for our final prototype.

Figure 33: Performance indexes at different air gap distances and different rotor thickness

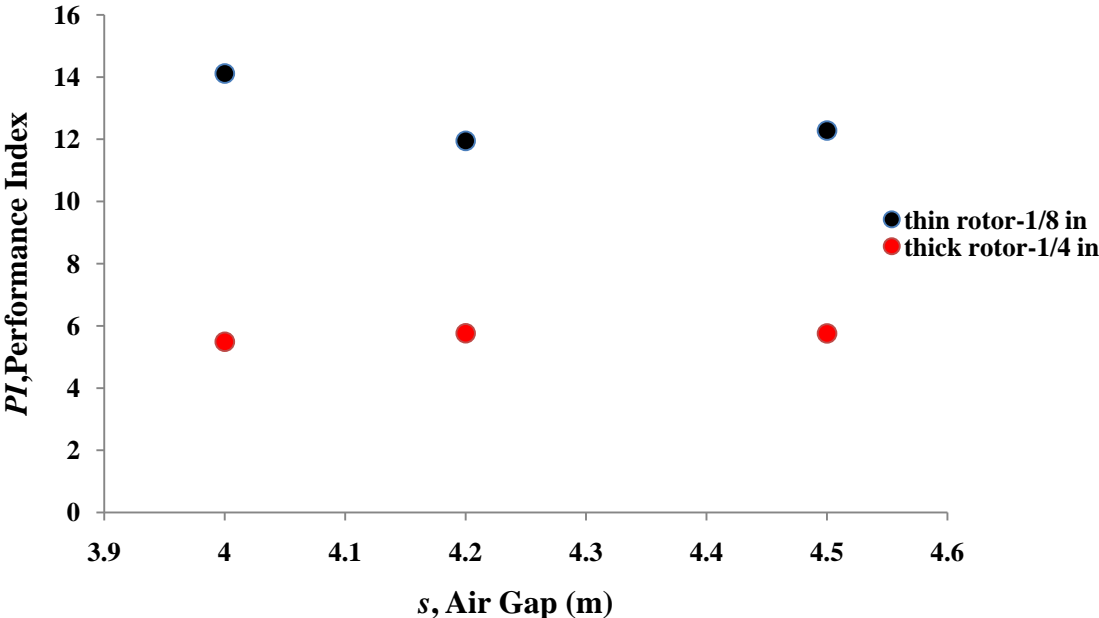
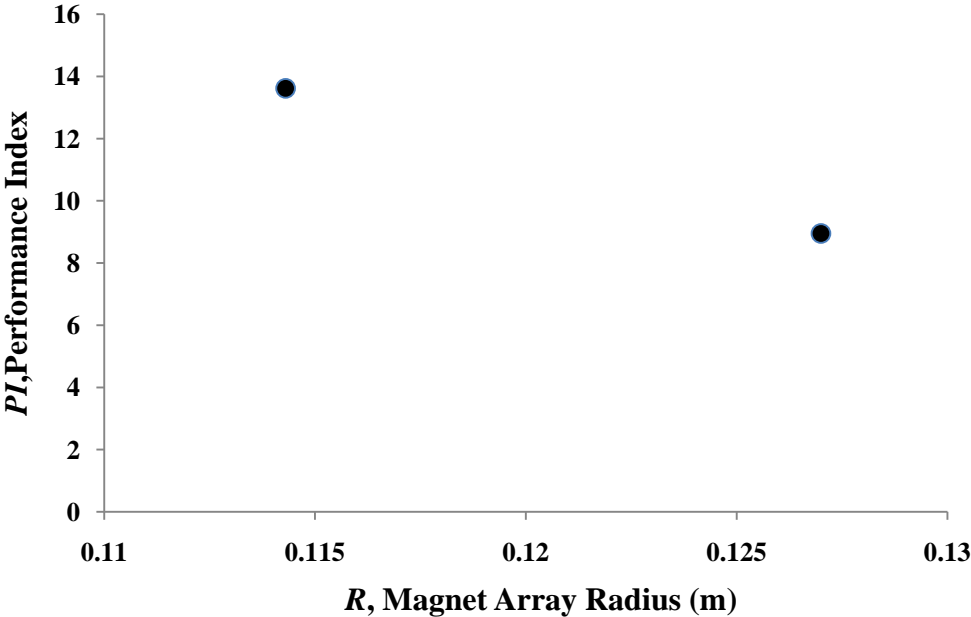


Figure 34 shows the functional relationship between the performance indexes and magnet array radii. The trend is that performance index decreases as the magnet array radius increases. The linearity cannot be determined.

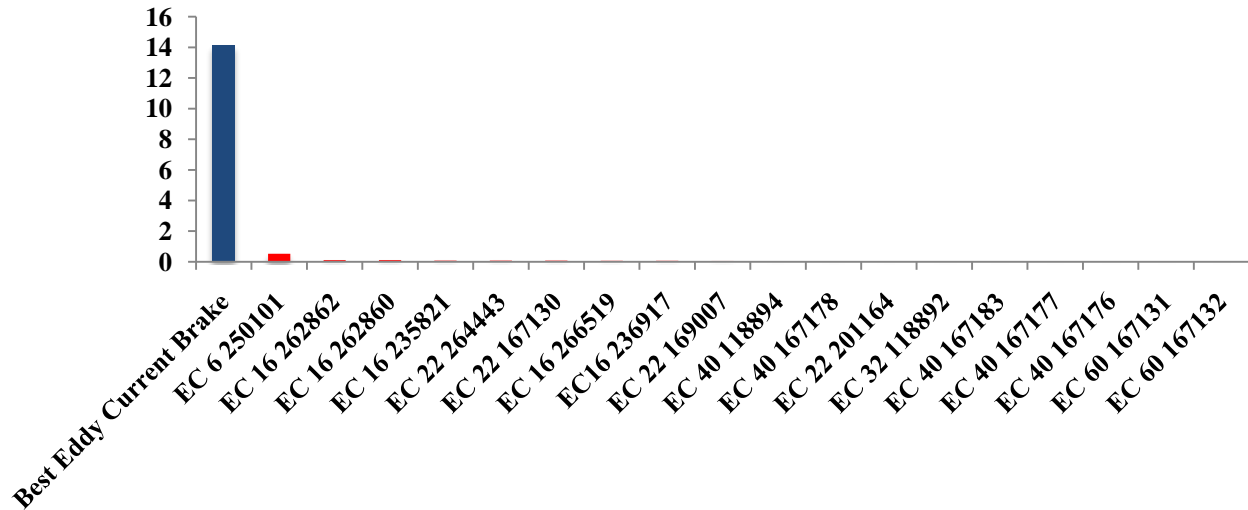
Figure 34: Performance indexes at different magnet array radius



12.3 Comparison of performance indexes

Figure 35 shows the comparison of performance indexes between our final prototype with other commercial DC motors. We conclude that our design meets our prescribed engineering specifications (co-existence of large torques and good backdrivability) very well since its performance index is much larger than those of current existing DC motors.

Figure 35: Comparison of performance indexes between our final prototype with other commercial DC motors



13 DESIGN CRITIQUE

The main problem with our design is that is difficult to adjust the shaft collars to move the rotor in and out. The first problem this design creates is that it is difficult to loosen the inside shaft collar because the hex key is attracted to the magnets. This problem could be solved by the use of a hex key made from a nonmagnetic material, for example stainless steel. The other problem is that when the device is fully assembled the shaft collar is fully enclosed in the stationary stator. The solution to this is to machine the stationary stator out of one block. The other problem was more of a manufacture problem than a design problem. When we manufactured the rotors we first cut them down to thickness and then drilled the whole in the center. This was a problem because it was difficult to get the thin plates to be perfectly vertical on the lathe. A better way to do this is to drill the whole into the stock and then cut it and machine it to thickness. This would ensure that the wall of the whole was perpendicular to the plate surface.

14 RECOMMENDATIONS

We recommend further experimental analysis of the eddy current brake performance in terms of its parameters. Experiments can be developed and employed that determine functional relationships between the brakes damping coefficient and its geometric parameters. By this means an optimum configuration can be determined. Further, possible design improvements can be employed to improve the versatility and configurability of the current model. One such

important improvement is the hub of the rotor. This can be improved in order to eliminate rotor run out allowing for small air gap configurations.

15 CONCLUSIONS

Team 16 developed a working desk top apparatus for use in experimentation of eddy current brake performance. Some experimental results are presented and should be continued. A performance index is suggested that can be used to compare the eddy current brake to existing electric motors. The current experimental results suggest that the eddy current motor would have to be driven at high speeds to show significant performance advantages over electric motors. This result may however be negated by experimentation and resulting optimized eddy current brake/motor configuration.

16 ACKNOWLEDGEMENTS

Thanks to all whose help has allowed us to achieve our goals.

17 INFORMATION SOURCES

Product benchmarking and patent searches were utilized to gain insight into successes and failings of existing eddy current motors and brakes. Since no direct analog to the current design exists, this process is limited in its usefulness.

17.1 Benchmarking

Eddy current brakes are a mature technology and there is a multitude of commercial devices in the market. However, all of such products found use electromagnetic coils to realize the magnetic field modulation (backdrivability), which is a fundamental design difference from the current design. In addition, no applications to haptic interfaces implementing eddy currents have been found. There is one scientific thesis describing the design of an eddy current brake for use as programmable viscous damper for haptic interfaces.

17.2 Patent Search

There were two patents that we found that are similar to the device that we are going to make in that they both control the braking force of an eddy current brake by moving permanent magnets in relation to a conductor to create eddy currents. The first patent is EP0497329 which is an eddy current drum brake. When you want to engage this brake you rotate permanent magnets so that their magnetic fields are pointed outward through the conductive drum to produce eddy currents. When you want to turn the brake off you rotate the magnets so that their magnetic fields go in a circle instead of going out through the brake drum. This design does not meet our design goals because the drum arrangement is not optimized for this layout. The second patent is US patent 6,659,237. This patent controls the strength of the eddy current braking by moving the magnets closer or further apart. This design does not meet our design goals because it can never be completely turned off.

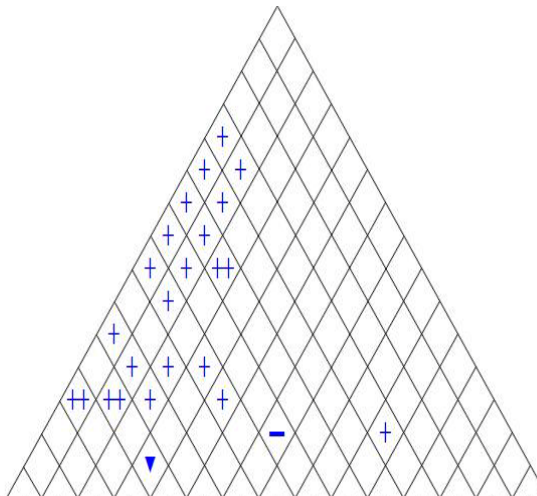
REFERENCES

- [1] A. Gosline and V. Hayward, “Eddy Current Brakes fro Haptic Interfaces, Design Identification and Control,” IEEE/ASME Transactions on Mechatronics, vol. 13, no. 6, pp. 66-677, 2008.
- [2] M. A. Heald, “Magnetic braking: Improved theory,” American Journal of Physics, vol. 56, no. 6, pp. 521–522, 1988.
- [3] K. Lee and K. Park, “Modeling eddy currents with boundary conditions by sing coulomb’s law and the method of images,” IEEE Transactions on Magnetics, vol. 38, no. 2, pp. 1333–1340, 2002.
- [4] E. Simeu and D. Georges, “Modeling and control of an eddy current brake,” Control Engineering Practise, vol. 4, no. 1, pp. 19–26, 1996.
- [5] Patent EP0497329
- [6] US patent 6,659,237
- [7] www.Maxonmotors.com
- [8] VIZIMAG Software
- [9] www.KJMagnets.com/calculator.asp

Appendix A: Gantt Chart



Appendix B: QFD



Legend		
	Strong Relationship	9
	Moderate Relationship	3
	Weak Relationship	1
	Strong Positive Correlation	
	Positive Correlation	
	Negative Correlation	
	Strong Negative Correlation	
	Objective Is To Minimize	
	Objective Is To Maximize	
	Objective Is To Hit Target	

Row #	Max Relationship Value in Row	Relative Weight	Weight / Importance	Demanded Quality (a.k.a. "Customer Requirements" or "Whats")	Quality Characteristics (a.k.a. "Functional Requirements" or "Hows")	Column #															Competitive Analysis (0= Worst, 5= Best)															
						1	2	3	4	5	6	7	8	9	10	11	12	13	14	15																
Direction of Improvement: Minimize (▼), Maximize (▲), or Target (X)						▲	▼	▼	▲	▼	▼	▼	X	▲	X	▲	X																			
						Torque generated when it is turned on [N*m]	Torque generated when it is turned off [N*m]	Inertia of the wheel [kg*m ²]	Magnetic field [T]	Magnetic field when turned off [T]	Wheel thickness [m]	Density of the wheel [kg/m ³]	Air gap [m]	Specific conductivity of the wheel [S/m]	Wheel radius [m]	Magnetic field area [m ²]	Number of magnets (#)			Stromag, Inc. Model No.19	Drive Source International, Inc Model AS 70	Competitor 2	Competitor 3	Competitor 4	Competitor 5											
1	9	38.5	5.0	Powerful to brake (brake) or to drive (motor)			0	0	0	0	0	0	0	0	0	0	0	0	5	4											▲	■				
2	9	38.5	5.0	Good backdrivability		0	0	0	0	0	0	0	0	0	0	0	0																			
3	9	23.1	3.0	Cheap		0	0																													
4																																				
5																																				
6																																				
7																																				
8																																				
9																																				
10																																				
Target or Limit Value																																				
Difficulty (0=Easy to Accomplish, 10=Extremely Difficult)						5	7	0	0	3	0	1	3	1	0	3	3																			
Max Relationship Value in Column						9	9	9	3	3	3	3	3	3	3	3	3																			
Weight / Importance						553.8	346.2	553.8	115.4	115.4	230.8	230.8	115.4	230.8	230.8	230.8	230.8																			
Relative Weight						17.4	10.9	17.4	3.6	3.6	7.2	7.2	3.6	7.2	7.2	7.2	7.2																			

Appendix C: Team Member Autobiographies

Hollowell, Thomas

I will receive my B.S. from Mechanical Engineering Department, University of Michigan at the end of winter 2010 term. I have special interest in vibrations and dynamics as well as manufacturing processes. I have worked for a family business manufacturing hydrostatic four-wheeled utility vehicles, which has contributed to my interest and experience in mechanical engineering. This vocation has also fostered an interest in all things mechanical, in a “gear head” sense. My primary hobbies consist of motorcycles and cars.

I am a native of Michigan, and come from a family of Wolverines. I have two siblings, a fraternal twin brother and a younger brother. I grew up twenty minutes from Ann Arbor in Plymouth, MI and attended Canton High School.

Post graduate education is a possibility. However, my plans immediately after graduation I plan to pursue employment and accrue experience.

Kahl, Justin

I was born in Kalamazoo, Michigan. My preteen years were spent in portage and I later moved to Mattawan, Michigan. In Mattawan, I went to Mattawan Consolidated Schools. During high school, I played football and wrestled. I earned many sports related awards including ironman, most improved and I was All-Conference honorable mention center. I was involved in the Catholic Community which kept me involved in many hours of community service. In terms of academic awards I was Mr. Calculus, and numerous drafting awards such as; Grand Prize Regional and 2nd in State for Mechanical Drafting, 1st in Region and 3rd in State for Architectural Drafting, and a few regionally placed CAD drawings. I'm in Sigma Chapter of the Theta Xi Fraternity at the University of Michigan. I'm in the College of Engineering in the Mechanical Engineering department. My interests include: my tech electives; Multi-Phase Flow, Intermediate Strength of Materials, Computational Fluid Dynamics, Manufacturing Processes and Thermodynamics II. Since I've been here I've done 2 years of research with Professor Ceccio and learned an insurmountable amount of knowledge from his team working on the hi-plate project. I was even invited down to Memphis to watch the hi-plate go under water at the LCC. It was both exhausting and marvelous, though I wish I could have seen more of the town (the dining is the best). I'm excited to see how we integrate this permanent magnet brake design in our Final Review and the Design Expose.

Stanczak, Matthew

I am from Troy Michigan and went to Athens High School. I have one sister who goes to the cross town rival Troy High School. This came about between my sophomore and junior years of high school my family moved from the east side of Troy to the west side of Troy and I just kept going to Athens.

The last three summers I have worked at DTE Energy, first in Data Integrity and then in the environmental department. During that time I have gotten the chance to visit several of the power plants in the area and spent a lot of time at Trenton Channel Power Plant and Monroe Power Plant. One of the most interesting things that I have seen while working at DTE is the

unloading of a train car filled with coal. Most people think that the way this is done is that a trapped door is opened in the bottom of the car and the coal spills out, But what actually happens is that they flip the entire coal car upside down and the coal spills out of the top.

I will graduate in December 2010 and will get a job that will hopefully be located someplace warmer than Michigan I have no plans to go to grad school at this time.

Wang, Yizhou

I will receive my B.S. from Mechanical Engineering Department, University of Michigan at the end of winter 2010 term. In the mean time, I will still receive an additional B.S. from my previous institute, UM-SJTU joint institute, Shanghai Jiaotong University. My current research interest is in computational material science, working with Prof. Anton Van der Ven in MSE Department. The current project is implementing first principle calculation and Monte Carlo simulation to predict material properties including both mechanical and chemical ones. We are interested in the materials that can be used as electrodes so we are calculating energies during the intercalation processes. Several successful results have been obtained on Li_xTiO_2 by now. We plan to publish our findings soon.

I have submitted my applications to some graduate schools and now am waiting for the admissions and offers. Quite different from what I am researching in, my declared interest field is system control because I find it quite interesting at the undergraduate level. Also I can see many opportunities and challenges in both commercial and scientific fields. My career goal is to be a professor because I find myself inspired to teach.

Because of my good GPA, I have received twice university honors and dean's list honors. Before transferring to UM, I received Chinese National Scholarship in my previous school which I treasure more.

APPENDIX D: DESIGN CHANGES SINCE DR3

There are two design changes from DR3 to the present design. The first is a change to the handle used for phasing. Previously the handle was only a rectangle but now the part where the user puts their hand is thinner so it is easier to use. The other change is there is a bearing block that is a separate piece from the stationary stator. We made this change so the small bearings would be further apart and there would be less force on them.

APPENDIX E: BILL OF MATERIALS

Dimensions	Material	Quantity	Description
5.5" diameter .12 inch thick	Aluminum 6061	1	Rotor for the eddy current effect
5.5" diameter .18 inch thick	Aluminum 6061	1	Rotor for the eddy current effect
5.5" diameter .25 inch thick	Aluminum 6061	1	Rotor for the eddy current effect
.25" diameter 6" length	Steel 4041	1	Axle for rotor
5.5" diameter .5" thick	Steel 4041	1	Rotating stator
1" diameter 2.5" length	Steel 1018	1	Rotating stator axle
.5"X6"X6"	Aluminum 6061	1	Holder for stator
.25"X2"X8"	Aluminum 6061	1	Handle
.5"X6"X6"	Steel 1018	1	Stationary Stator
3"diameter 2" length	Aluminum	1	Spacer
1/4-20 6" cap screw	Steel grade 8	1	Maintain distance between stators
1/8" X 1" dowel pins	Steel	4	Transmit torque from handle to axle and axle to rotating stator
1" ID 1.25" OD 1/32 thickness washer	Hard Fiber	2	Separate handle from bearing and rotating stator from bearing
1/4-20 flange nuts	Steel	12	Hold stators in place
.25" ID .5" OD .125" Thickness ball bearing	Stainless Steel	2	Let the rotor axle spin free
1" ID 1 31/32" OD 5/8 Thickness thrust bearing	Steel	2	Support the rotating stator against axial loads
1" ID 1.25" OD .5" length thrust bearing	Bronze SAE 841	1	Support the radial weight of the rotating stator
1/4" keyless bushing	Steel	1	Connect the rotor to the rotor axle
1.25" diameter pulley	Delrin	1	Attach test weight
Bolts 1/4-20 1"	Steel	2	Connect rotating stator to axle and handle to axle
Bolts 1/4-20 1"	Steel	2	Connect spacer to stator holder
Shaft collar 1/4 ID	Steel	2	Hold the rotor axle in place
Shaft collar 1" ID	Steel	1	Hold the rotating stator axle in place

APPENDIX F: MATERIAL SELECTION

1 MATERIAL SELECTION

The section presents analyses on material selection in both functional and environmental perspectives. They are parts of group assignments required in ME450 Senior Design course.

1.1 Functional Performance

The functional performance analyses are conducted during the selection of materials used to make our rotor and two stators. By use of Cambridge Engineering Selector (CES), we are able to search among all bulk materials for the best candidates according to our prescribed criteria or so-called material indices. The selected materials will go further through the environmental performance analyses, which will be shown in the next section.

1.1.1 Function, objective and constraints

The two major components that we are going to analyze the functional performance are the rotor and the stator. Other than these, the assembly only needs some little components, such as fasteners, load-support bearings. The rotor, which is supposed to free rotate between two stators with magnets attaching on, is where eddy currents generate. To tell apart the viscous damping forces resulted from eddy current effect and magnetic attracting forces, we would like to select a non-magnetic material for the rotor. Also the material of the rotor is expected to have a small density, remembering that we are seeking low moment of inertia from it. The stator is where we attach numerous magnets in an optimized pattern. The material of the stator is wanted to be magnetic for convenience of fastening magnets, since the orientation or position of magnets is subject to chance to achieve best brake performance. Other common requirements or constraints of material selection are cheap (cost), stiff (rigidity), easy to machine (process compatibility) etc.

1.1.2 Material indices

The property limit is the magnetism of materials of these two components specified in the section above. The material index for rotor, M_r , is selected to be the ratio of the specific conductivity to the density. Maximizing this index will result in a maximized brake torque.

$$M_r = \sigma / \rho \quad \text{Equationxxx}$$

This analysis has been discussed and presented in Section 5.2.

The material index for stator, M_s , is selected to be the ratio of square root of the Young's modulus to the density since minimum weight and stiffness are prescribed.

$$M_s = E^{1/2} / \rho \quad \text{Equationxxx}$$

1.1.3 Final choice of materials and other competitors

Figure F1 shows the graph stage of selection of rotor materials with a limit in price of 5 dollars per pound. The dashed guidelines have slopes of 1. The closer to the upper left, the better the material fits our design. Five choices are labeled in the figure. Among these, we select aluminum because of cheapest price and availability.

Figure F2 shows the graph state of selection of stator materials with a limit in price of 3 dollars per pound. The dashed guidelines have slopes of 1. The closer to the upper left, the better the material fits our design. Five choices are labeled in the figure. Among these, we select stainless steel because of cheapest price and availability.

Figure F1: Rotor materials selection

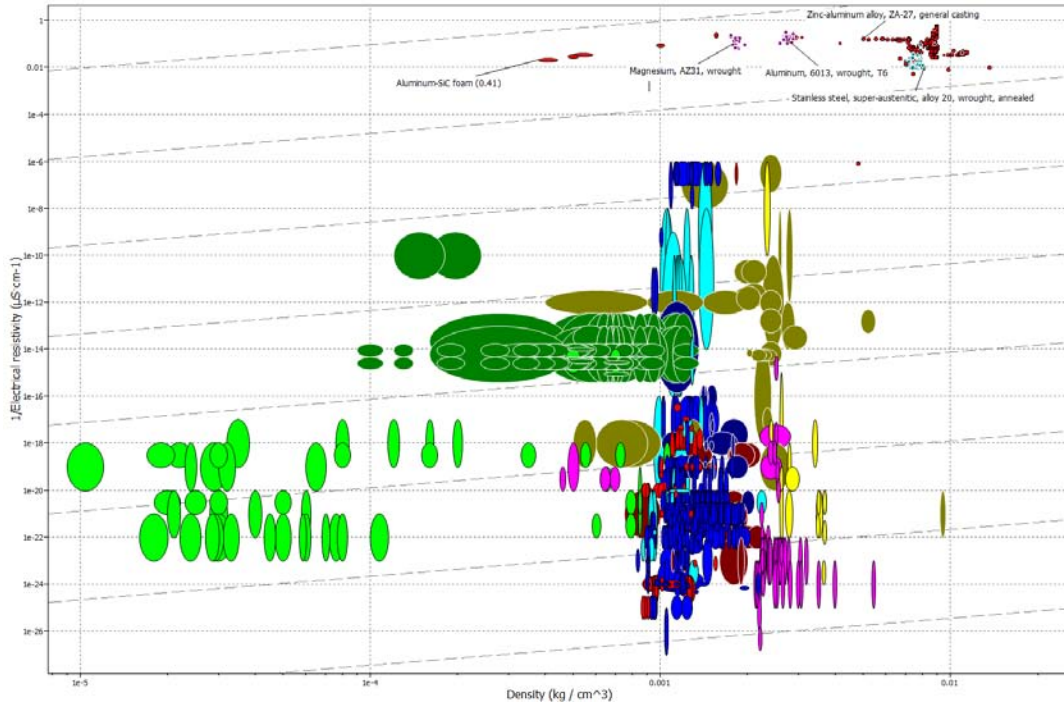
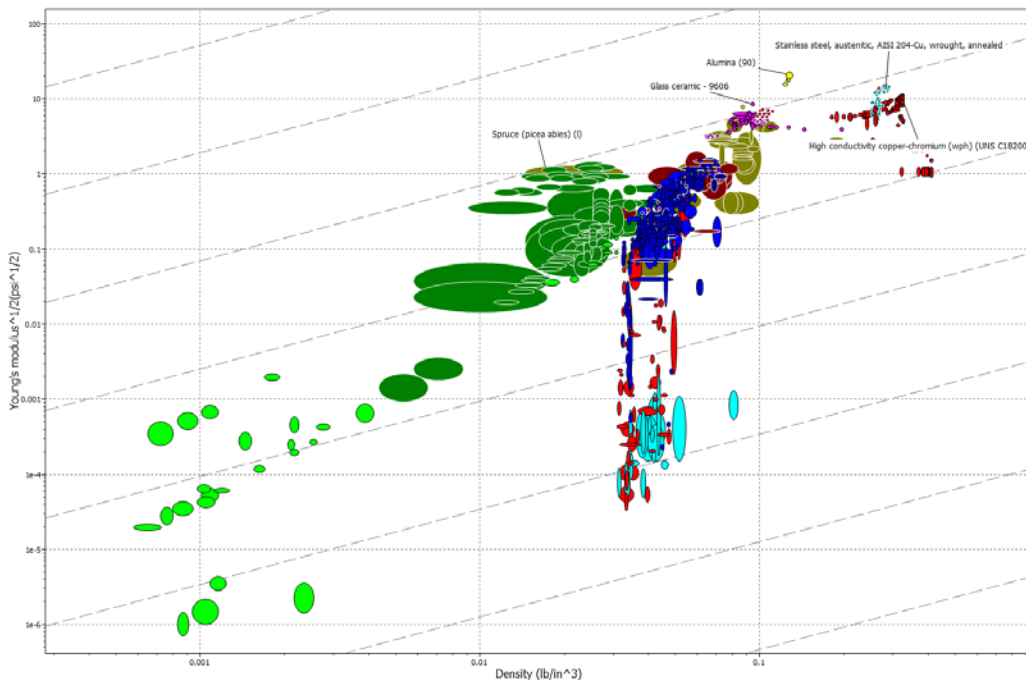


Figure F2: Stator materials selection



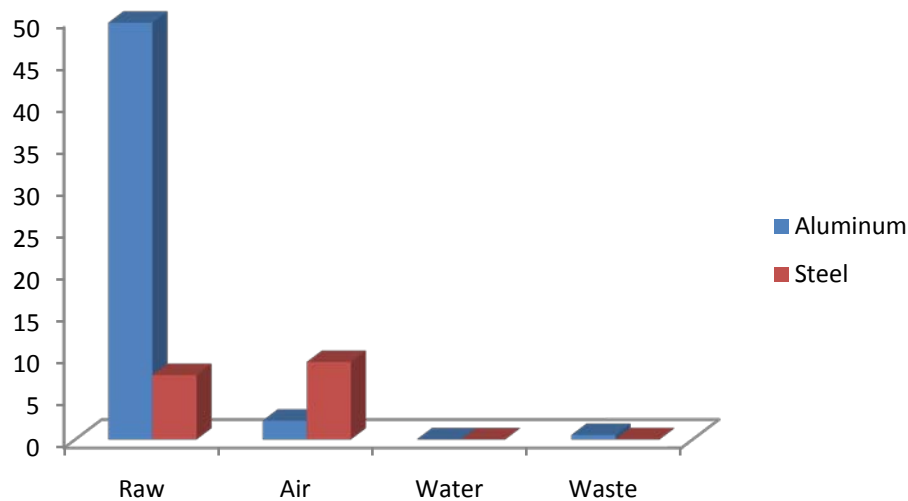
1.2 Environmental Performance

The environmental performance analyses are conducted for these two selected materials and the results are shown in this section. With the help of SimaPro software, we are able to precisely calculate the impact of use of these amounts of materials, and then compare which dominates in the pollution.

1.2.1 Calculation of total emissions

Emissions are categorized into raw, air, water and waste. SimaPro calculated the amount of emissions in each of the category. The materials we chose in SimaPro were 1 kilogram aluminum (Al99I) and 6 kilogram steel (X10CrNiMoNb I). The results are shown in Figure F3 in bar graph. Emissions in raw and air are relatively significant, compared with in water and waste. “Water, unspecified natural origin” contributed most in emissions of use of aluminum, whose amount was 48 kg. The significance of the amount of emission leads us to consider whether the selection of material should be re-evaluated later if the design is put into massive production.

Figure F3: Bar graph of air emission, water emission and (solid) waste



1.2.2 Results of Eco-indicator 99 calculation

The method, Eco-indicator 99, as a damage-oriented approach implemented in SimaPro, calculated the environmental impact of material usage, which included not only energy content, but also such things as the emission of a toxic by-product, the difficulty of recycling, and the resistance to biodegrading. The latter ones are usually ignored, but are the real environmental threat under certain circumstances. In Figure F4, the damage models in the software are represented in a schematic way.

Figure F4 Detailed representation of the damage model in Eco-indicator 99

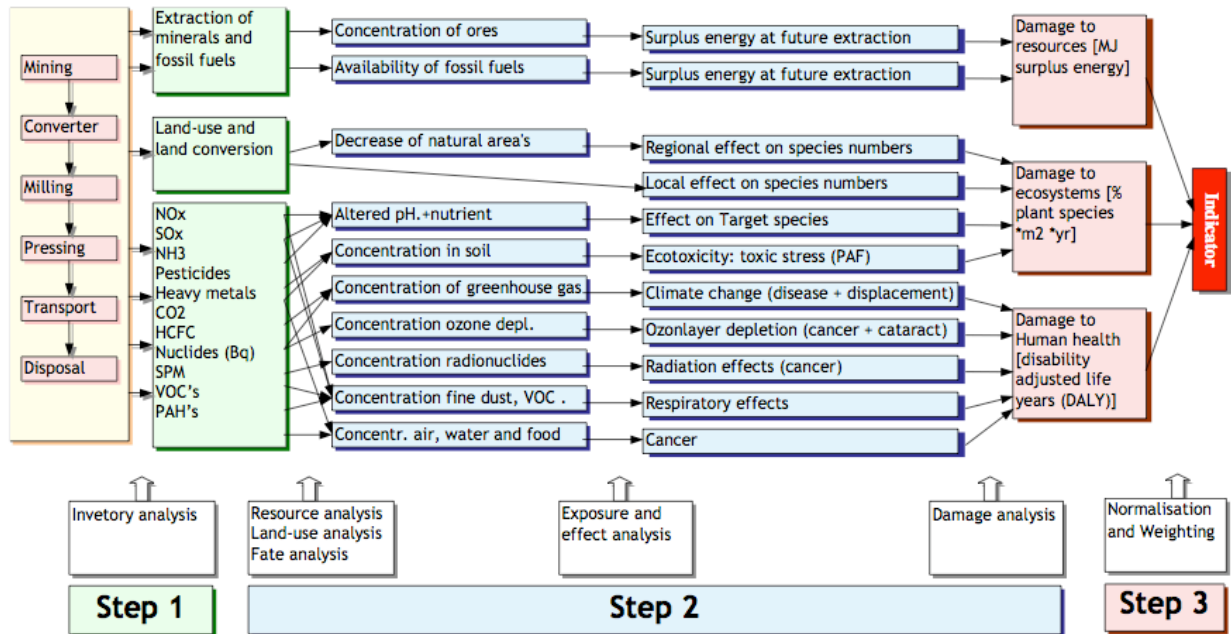


Figure F5 shows the impact category indicator results. The lengths of bars indicate which material dominates in each of the EcoIndicator 99 damage classifications. As the result shows, the use of steel dominates in most categories, except carcinogens and ozone layer.

Figure F5: Relative impacts in disaggregated damage categories

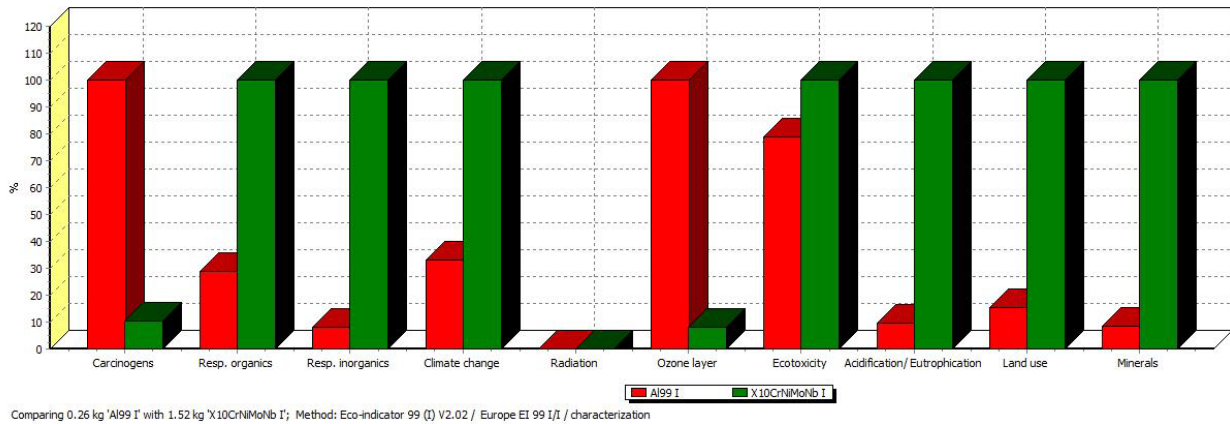


Figure F6 shows the normalized impact in three damage categories: human health, ecosystem quality and resources. The normalization process waives the weighting effect in comparison. As the result show, the use of steel has more significant impact in all of three damage categories. “Resources” is most likely to be important among all three damage meta-categories based on the EI99 point values. Figure F7 is the single-scored graphical result, which has the same indications.

Steel has a higher EcoIndicator 99 “point value” shown in the figures. We also think that when the life cycle of the whole product is considered, this result holds.

Figure F6: Normalized score in human health, eco-toxicity, and resource categories

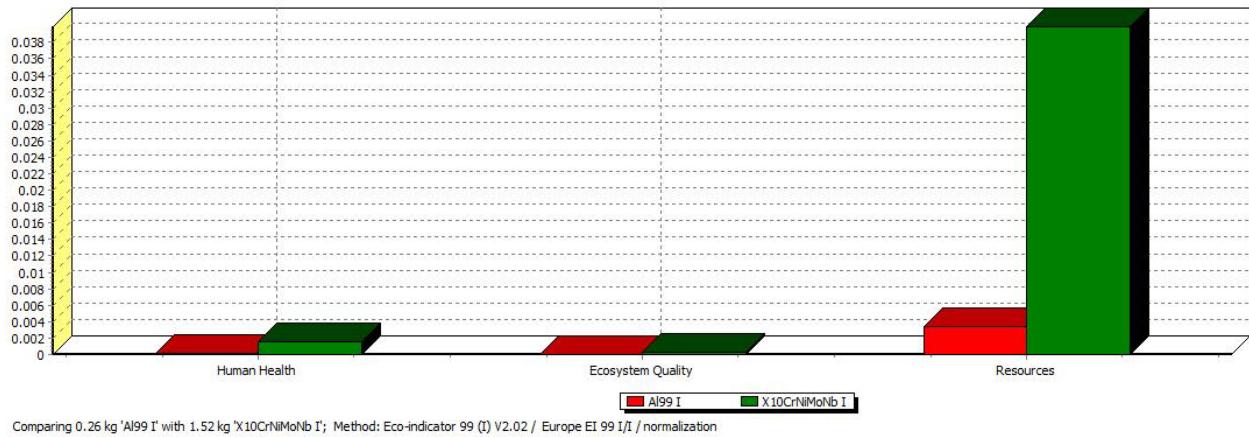
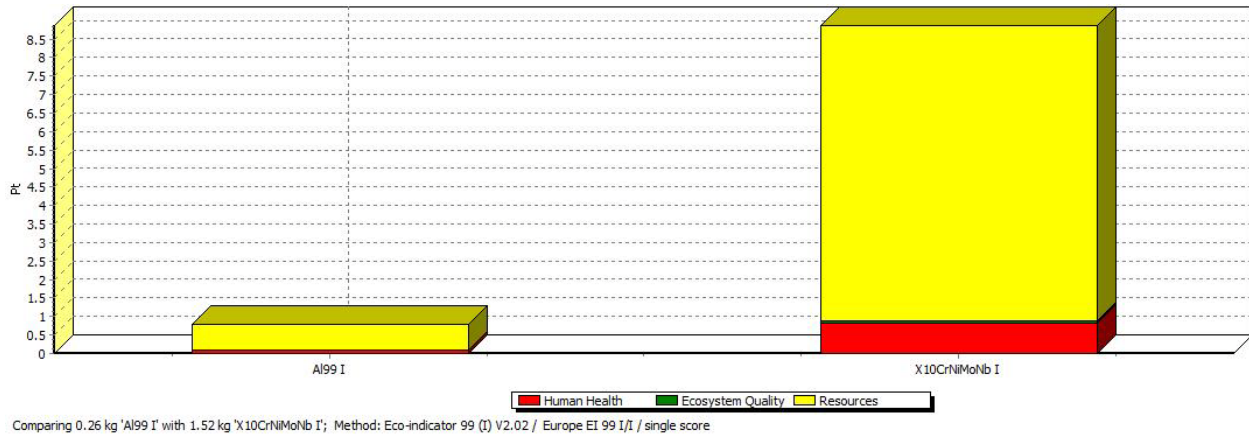


Figure F7: Single-scored impact assessment



1.2.2 Consideration of re-selection of materials

At this time, we are not considering reselection of materials. We might probably do that in the case of massive production.

1.3 Manufacturing Processes

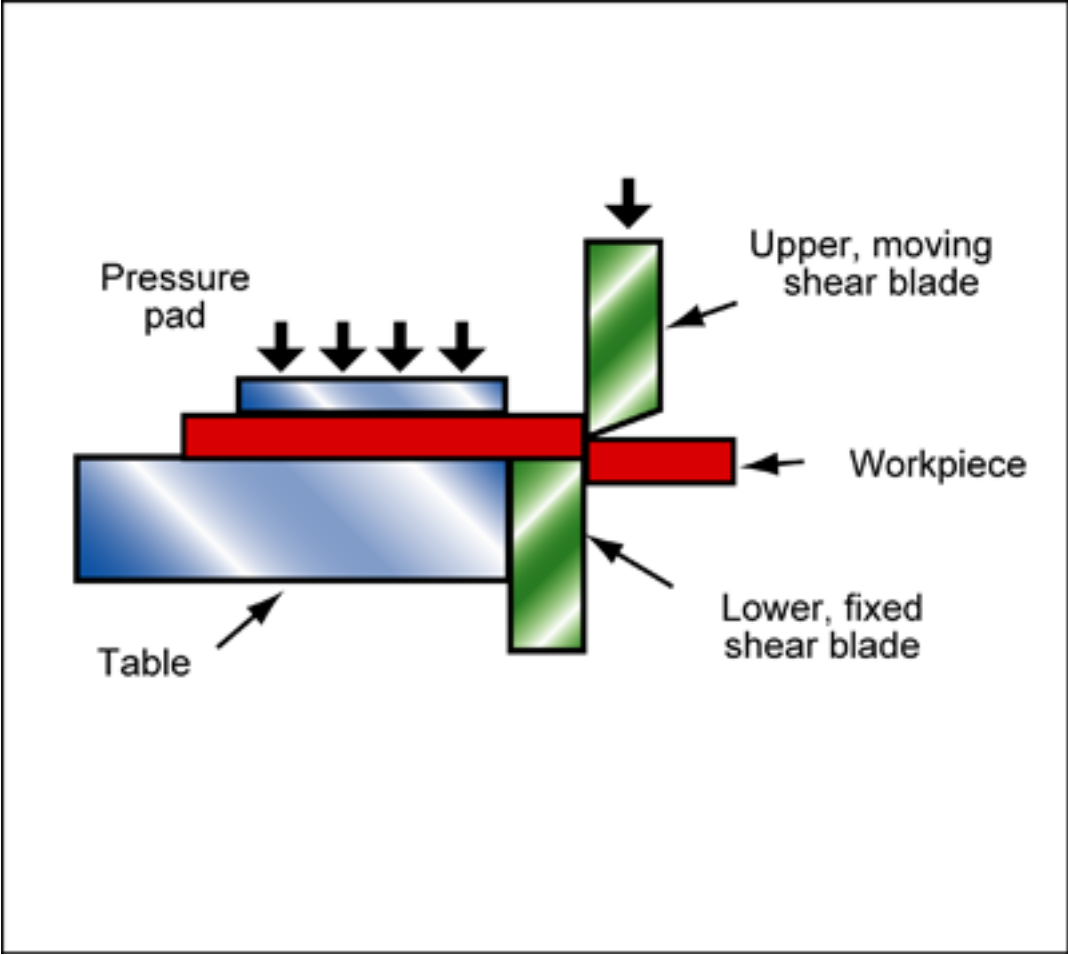
A feasible market demand for the ECB is on the order of 1000 because its primary use is for research. Thus, demand is limited to academia.

1.3.1 Stainless Steel Stator

The stator is 6” x 6” x 0.5” plate of stainless steel. First, the bulk material needs to be shaped and then the stator needs to have holes machined in it. Cambridge Engineering Selector (CES) was

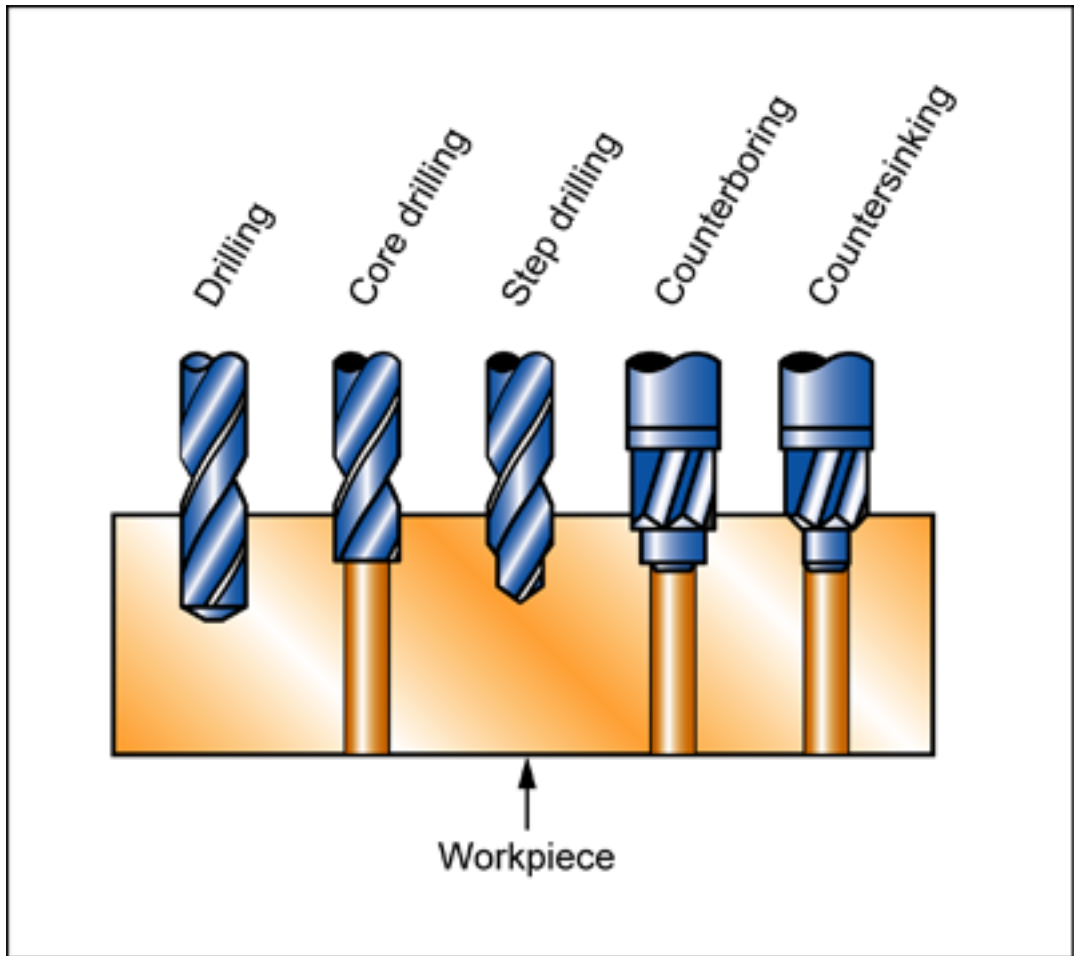
used to search all manufacturing processes in order to best select the method by which to mass produce the stator. The bulk material will be bought from a metal supplier with 24' X 6" x 0.5" dimensions. Thus, the shaping process consists of one cut per part. CES provided a list of possible processes meeting the manufacturing constraints including: low cost, medium speed, medium volume, stainless steel, and 0.5" thick cut. From this list guillotining was selected primarily due to its low set up cost. Figure F8 shows the selected process.

Figure F8: Guillotine process used for cutting of bulk stator material



The second stator manufacturing process consists of machining holes. CES was used to select the best process. Drilling was selected due to its low cost and the simple geometry of the stator. A CNC mill could be used to increase volume. Figure F9 shows the selected process.

Figure F9: Drilling process used for cutting of bulk stator material



1.3.1 Aluminum rotor

The rotor is a 0.125" thick, 5.5" diameter disk of aluminum. First, the bulk material needs to be shaped and then the rotor needs to have a center hole accurately machined in it. Cambridge Engineering Selector (CES) was used to search all manufacturing processes in order to best select the method by which to mass produce the rotor. The bulk material will be bought from a metal supplier with 24' X 5.5" diameter dimensions. Thus, the shaping process consists of one cut per part. CES provided a list of possible processes meeting the manufacturing constraints including: low cost, medium speed, medium volume, stainless steel, circular part, and 0.125" thick part. From this list parting was selected primarily due to its low tooling cost. Figure F10 shows the selected process.

The second rotor manufacturing process consists of machining and accurate center hole. CES was used to select the best process. Boring was selected due to its low cost, good accuracy and the circular geometry of the stator. A CNC lathe could be used to increase volume by combining the parting and boring processes. Figure F10 shows the selected process.

Figure 10: Parting and boring process used for manufacturing of aluminum rotor

